Received: 8 April 2026 | Revised: 9 June 2026 | Accepted: 11 June 2026

DOI: 10.1111/joa.70201

Journal of Anatomy | ANATOMICAL SOCIETY WILEY

ORIGINAL ARTICLE

Musculo-skeletal variation in the forelimb of two highly specialised diggers (genus *Talpa*)

Estelle Klein[1] | Anthony Herrel[2,3,4,5] | Céline Houssin[1] | Arnaud Delapre[1] | Violaine Nicolas[1] | Damien Chablat[6] | Mathieu Porez[6] | Raphaël Cornette[1]

[1]Institut de Systématique, Evolution, Biodiversité (ISYEB), UMR 7205, Muséum National d'Histoire Naturelle, CNRS, SU, EPHE, UA, Paris, France

[2]Mecanismes Adaptatifs et Évolution (MECADEV), Muséum National d'Histoire Naturelle, Paris, France

[3]Department of Biology, Evolutionary Morphology of Vertebrates, Ghent University, Ghent, Belgium

[4]Department of Biology, Functional Morphology Laboratory, University of Antwerp, Antwerp, Belgium

[5]Naturhistorisches Museum Bern, Bern, Switzerland

[6]Laboratoire Des Sciences du Numérique de Nantes (LS2N), UMR 6004, CNRS, Nantes Université, École Centrale Nantes, IMT Atlantique, Nantes, France

Correspondence
Estelle Klein, Institut de Systématique, Evolution, Biodiversité (ISYEB), UMR 7205, Muséum National d'Histoire Naturelle, 57 rue Cuvier 75005, Paris, France.
Email: estelle.klein@mnhn.fr

Abstract

The forelimbs of mammals are involved in many crucial behaviours for an animal's ecology, including locomotion. It has been shown that forelimb morphology and locomotor mechanisms are greatly impacted by functional constraints induced by the properties of the media across or in which the animal moves. These functional constraints are thought to drive an important part of bone shape, as bone directly remodels in response to both muscle and external forces. Due to its anatomical particularities, the forelimb of fully fossorial moles is of particular interest to better understand fossorial adaptations and has already been studied extensively. Recently, some studies focusing on two European mole species, *Talpa europaea* and the recently described *Talpa aquitania*, highlighted inter and intraspecific variations in the inner ear and forelimb bones morphology, which could be linked to locomotor performances. To better understand the specificity of their fossorial adaptations, we focus, in the present study, on these two species' musculature. Performing anatomical dissections, and in accordance with the literature, we provided a redescription of 39 extrinsic and intrinsic muscles inserting on the forelimb bones. We also made a quantitative comparison of muscles features, both at the inter and intraspecific level. Especially, we focus on muscle Physiological Cross-Sectional Area (PCSA), a measure considered as a good estimator of the force-producing capacity of a muscle. Finally, to investigate relationships between bone shape and muscle force, we quantified covariations between shape data and muscle PCSA. Our results highlighted inter and intraspecific (in *T. aquitania*) variations in muscle force-producing capacity, which is consistent with the studies of the inner ear and forelimb bones. Focusing on the relationship between muscle PCSA and shape of ulna and humerus, we showed that shoulder extensors, carpal/digital extensors, and carpal/digital flexors' PCSA were highly integrated with humerus shape and that elbow extensors' PCSA were highly integrated with the ulna shape. These results are rather consistent with insertion sites of these muscles on bones.

KEYWORDS
anatomical dissections, fossorial adaptations, morpho-functional, muscles, *Talpa*

1 | INTRODUCTION

Limbs are the main structures used by terrestrial mammals for locomotion, which is a crucial behaviour for an animal's ecology. Indeed, social and feeding behaviours such as foraging, searching for mating partners, pursuing prey, or avoiding predators are dependent on locomotion (Biewener & Patek, 2018; Böhmer et al., 2021). These diverse functions involve the forelimbs, which in mammals often display a greater number of functional roles than the hind limb (Fabre et al., 2015; Polly & Hall, 2007; Rothier et al., 2023). Despite supporting the individual weight, the forelimb must also resist the stresses and strains induced during locomotion (Fabre et al., 2015). Forelimb morphology is thus greatly impacted by functional constraints induced by the properties of the media across or in which the animal moves (Biewener & Patek, 2018). Wolff's law stipulates that these functional constraints impact bone shape, as bone is a living tissue that dynamically adapts to the loads it experiences (Wolff, 1892). It has been shown that these constraints drive an important part of the bone shape, as bone directly remodels in response to both muscle and external forces (Currey, 2002, 2003; Sharir et al., 2011). Indeed, the size of muscle insertions and the strength and curvature of bones are influenced by muscle volume and strength (Brassard et al., 2020; Cornette et al., 2015). Therefore, mammal limbs have adapted to constraints imposed by habitat use and locomotion, showing morphological specialisations reflecting the diversity of their lifestyle and environment (Polly & Hall, 2007).

The fossorial lifestyle of *Talpa* species is of particular interest due to the strong constraints imposed by the subterranean environment. According to Nevo (1979), this environment corresponds to a microclimatically stable system. Furthermore, moles must move through a dense medium requiring powerful forelimbs to shear and shift the soil (Abe, 2001). Their morphology is adapted to digging and several convergences can be observed between species. Notably, moles have a fusiform body shape, a long snout but short neck, reduced eyes and external ears protecting them from the substrate, and short limbs (Edwards, 1937; Marchetti et al., 2024; Nevo, 1979; Rohlf et al., 1996). In addition, moles have soft fur that can move in any direction, thus minimising abrasion on burrow walls and improving movement through tunnels (Marchetti et al., 2024). However, the forelimb displays the most extreme specialisations (Figure 1). Bones show a highly derived shape compared with non-digging mammals as they are generally shorter, larger and more robust and exhibit many prominent processes for the attachment of powerful muscles which move the limb (Edwards, 1937; Hutchison, 1968). Furthermore, Castiella et al. (1992) underlined the specific orientation and position of the forelimb and its bones. For instance, due to this orientation, what is traditionally on the lateral side of the humerus, ulna and radius is oriented medially, and conversely, in moles.

Due to its particularities, the forelimb in *Talpa europaea* has been studied extensively (Campbell, 1939; Castiella et al., 1992; Freeman, 1886; Jullien, 1967; Whidden, 2000; Yalden, 1966). Several authors described the extrinsic and intrinsic muscles of the limb but focused mostly on the shoulder (Campbell, 1939; Castiella et al., 1992; Freeman, 1886). Reed's work (1951) dealt with the whole limb but did not include *Talpa* species. Yalden (1966) simplified his work and added more illustrations but did not provide muscle descriptions and rather discussed functional interpretations from his observations. Moreover, as the new cryptic species *Talpa aquitania* was only distinguished from *T. europaea* populations based on mitochondrial DNA in 2014 (Hugot et al., 2014) and described in 2017 (Nicolas et al., 2017), it is unclear which of the two species was described by previous authors.

These two species co-occur in south-western Europe in allopatric or parapatric distributions: *T. aquitania* is present in northern Spain and south-western France and *T. europaea* is widely distributed from north-eastern France to Russia (Nicolas et al., 2017; Wilson & Mittermeier, 2018). In France, *T. aquitania* and *T. europaea* have mostly allopatric geographical distribution, even if small areas of contact between them are present in the Pyrenees mountains, the Var department and around the Loire river (Nicolas et al., 2021). The factors explaining their geographic distribution are still incompletely understood even though some hypotheses on the role of

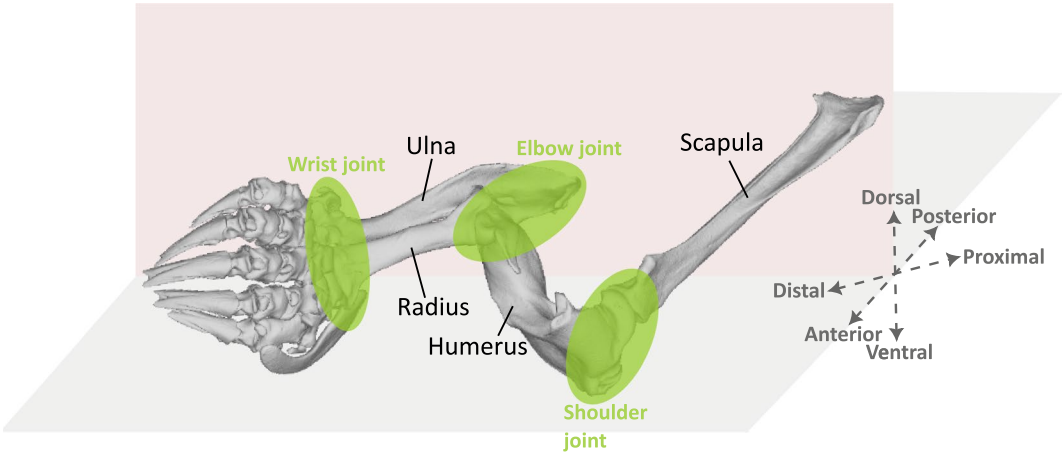

FIGURE 1 Illustration of *Talpa aquitania*'s right forelimb anatomy (specimen MNHN-ZM-2018-2240).

climate, food resource abundance, and historical factors have been suggested (Nicolas et al., 2021).

Despite the morphological convergences of *Talpa* species, Costes et al. (2023) highlighted morphological variation in the humerus and ulna between three species, *T. europaea*, *T. aquitania*, and *T. occidentalis*, as well as intraspecific variations between two populations of *T. aquitania* (from the Gironde and Aveyron departments in France). These shape variations were mainly found in muscle attachment sites, suggesting that variation in muscles exists. Therefore, it is relevant to investigate the forelimb musculature of these species. Here we focused on the two French species, *T. europaea* and *T. aquitania*. We also compare individuals of the two populations of *T. aquitania* for which Costes et al. (2023) described anatomical variation in the forelimb bones.

Here, we first provide a redescription of muscles of the forelimb based on the literature available and on anatomical dissections of *T. europaea* and *T. aquitania*. Second, we qualitatively and quantitatively compare the muscle architecture of the forelimb muscles of the two species and for the two *T. aquitania* populations. We calculated the Physiological Cross-Sectional Area (PCSA) for each muscle and made comparisons, using multivariate analyses, at both the inter and intraspecific levels. Finally, to investigate relationships between bone shape and muscle PCSA, we quantified covariations between shape and PCSA.

2 | MATERIALS AND METHODS

2.1 | Specimens

All specimens came from the collections of the National Museum of Natural History of Paris and were preserved in a 70% aqueous ethanol solution. Nine forelimbs of nine adult specimens were dissected, including three specimens of *T. europaea*, three of *T. aquitania* captured in Gironde, and three of *T. aquitania* captured in Aveyron (Table 1). These specimens were selected as Costes et al. (2023) highlighted morpho-functional variations of their humerus and ulna, both at an inter and intraspecific level (for *T. aquitania*). No specimens were killed for this study.

Thirty-nine muscles corresponding to the intrinsic and extrinsic muscles of the forelimb were identified and extracted. Their origins and insertions as well as their functions are listed below

TABLE 2 Extrinsic and intrinsic forelimb muscles classification in functional groups, following Edwards (1937), Rose et al. (2013), Böhmer et al. (2021) and our observations. t.b.: Triceps brachii.

Functional groups	Muscles
Scapular retractors	*Spinotrapezius*
Scapular abductors	*Serratus ventralis*
Scapular protractors	*Rhomboideus capitis, rhomboideus cervicis, omotransversarius*
Scapular adductors	*Rhomboideus capitis, rhomboideus cervicis, rhomboideus profundus*
Shoulder extensors	*Cleidodeltoideus, acromiodeltoideus*
Shoulder flexors	*Spinodeltoideus, triceps brachii caput longum*
Humeral abductors	*Latissimus dorsi, pectoralis superficialis, pectoantebrachialis, pectoralis major, pectoralis minor, teres major, subscapularis*
Humeral adductors	*Cleidodeltoideus, acromiodeltoideus, spinodeltoideus, supraspinatus, biceps brachii*
Elbow extensors	*Epitrochlearis, t.b. caput longum, t.b. caput laterale, t.b. caput mediale, anconeus, t.b. caput accessorium*
Elbow flexors	*Biceps brachii, pronator teres, brachialis*
Digital extensors	*Extensor digitorum lateralis, extensor digitorum communis, extensor digiti I and II*
Carpal extensors	*Extensor carpi radialis, extensor digitorum lateralis, extensor digitorum communis, extensor digiti I and II, abductor pollicis*
Digital flexors	*Flexor digitorum profundus, flexor digitorum superficialis*
Carpal flexors	*Flexor carpi ulnaris, flexor digitorum superficialis, palmaris longus*

TABLE 1 Species, sample location, and sex for each specimen.

Species	Specimens	Sex	Departement	Location	Coordinates N	Coordinates W
T.aquitania	MNHN-ZM-2018-2242	F	Aveyron	Vines/Cantoin	44.8550	2.8090
T.aquitania	MNHN-ZM-2018-2244	M	Aveyron	Vines/Cantoin	44.8550	2.8090
T.aquitania	MNHN-ZM-2018-2245	F	Aveyron	Vines/Cantoin	44.8550	2.8090
T.aquitania	MNHN-ZM-2017-2258	F	Gironde	Landiras	44.5667	−0.4167
T.aquitania	MNHN-ZM-2017-2261	M	Gironde	Cestas	44.7333	−0.6833
T.aquitania	MNHN-ZM-2017-2271	M	Gironde	Saint-Sulpice-et-Cameyrac	44.9108	0.3894
T.europaea	MNHN-ZM-2018-605	F	Ille-et-Vilaine	Saint-Lunaire	48.5821	−1.6699
T.europaea	MNHN-ZM-2018-606	F	Ille-et-Vilaine	Saint-Lunaire	48.5821	−1.6699
T.europaea	MNHN-ZM-MO-1993-3218	M	Essonne	Vaugrineuse	48.6031	2.1201

TABLE 3 Description of origin and insertion sites and functions of forelimb muscles of *T. europaea* and *T. aquitania*. Remarks indicating differences with previous work are added in the last column. t.b.: Triceps brachii.

Muscle name	Origin	Insertion	Function.s	Remarks
1. *Cleidomastoideus* (Figure 2)	Medial side of articular facet of the sterno-Clavicular joint (clavicle)	Mastoid process of temporal bone (skull)	Neck rotator	Considered as one muscle with m. *sternomastoideus*, m. *sternocleidomastoideus* in Jullien, 1967 and Castiella, 1992
2. *Spinotrapezius* (Figure 3)	Spinous processes of lombar vertebrae anterior to m. *latissimus dorsi* origin	Posterior to infraspinous fossa and m. *spinodeltoideus* origin (scapula)	Scapular retractor	Posterior part of m. *trapezius* in Jullien, 1967 and Castiella, 1992; m. *trapezius posticus* in Whidden, 2000
3. *Rhomboideus capitis* (Figures 2 and 3)	Most anterior part of parietal bone (skull)	Postero-laterally to supraspinous fossa (scapula)	Neck elevator, scapular adductor and protractor	One of the three parts of m. *rhomboideus* in Jullien, 1967; m. *rhomboideus pars occipitalis* in Castiella et al., 1992
4. *Rhomboideus cervicis* (Figure 3)	Spinous processes of cervical vertebrae	Posterior to supraspinous fossa and m. *rhomboideus capitis* insertion (scapula)	Scapular adductor and protractor	One of the three parts of m. *rhomboideus* in Jullien, 1967; m. *rhomboideus pars cervicalis* in Castiella et al., 1992
5. *Rhomboideus profundus* (Figures 2 and 3)	Parieto-occipital suture, posterior to m. *rhomboideus capitis* origin (skull)	Via the interscapular ligament, posteriorly to *subscapularis* fossa and m. *serratus ventralis* insertion (scapula)	Scapular adductor	One of the three parts of m. *rhomboideus* in Jullien, 1967; m. *rhomboideus pars dorsalis* in Castiella et al., 1992; m. *rhomboideus posticus* in Whidden, 2000
6. *Serratus ventralis* (Figure 3)	Lateral surfaces of ribs	Posterior to m. *teres major* tendon and to *subscapularis* fossa (scapula)	Scapular abductor	m. *serratus anterior* in Jullien, 1967 and Castiella et al., 1992; divided in m. *serratus ventralis cervicis* and m. *serratus ventralis thoracis* in Whidden, 2000
7. *Omotransversarius* (Figure 3)	Transverse processes of cervical vertebrae	Lateral to *supraspinous* fossa, ventrally to m. r. *capitis* insertion (scapula)	Scapular protractor	m. *levator scapulae* in Jullien, 1967 and Castiella et al., 1992
8. *Subclavius pars Clavicularis* (Figure 2)	Antero-ventral tip of the manubrium (sternum)	Medial side of anterior process (clavicle)	Clavicle retractor, shoulder joint stabiliser	One of the three head of m. *subclavius* in Whidden, 2000
9. *Subclavius pars scapularis* (Figure 3)	Manubrium, dorsally to m. *subclavius* origin (sternum)	Medial side of acromion process (scapula)	Shoulder joint stabiliser	m. *costoscapularis* with two head in Jullien, 1967; m. *costoscapularis pars ventralis* and *pars dorsalis* in Castiella et al., 1992; one of the three head of m. *subclavius* in Whidden, 2000.
10. *Latissimus dorsi superficialis*	Superficial sheet of m. *latissimus dorsi*, inserting into the integument above the muscle		Humeral abductor	
11. *Latissimus dorsi* (Figure 4)	Spinous processes of lombar vetebrae	Lateral border of the *teres* tubercle (humerus)	Humeral abductor	

TABLE 3 (Continued)

Muscle name	Origin	Insertion	Function.s	Remarks
12. *Pectoralis superficialis*	Superficial sheet of Mm. *pectorales*, inserting into the integument above the muscles		Humeral abductor	Mm. *pectoralis* subdivided in m. *pectoralis major* and m. *pectoralis minor* in Jullien, 1967; one muscle m. *pectoralis* subdivided in five parts in Castiella et al., 1992; Mm. *pectoralis* subdivided in m. *pectoralis superficialis pars anticus*, m. *pectoralis superficialis pars posticus*, m. *pectoralis abdominalis*, m. *pectoralis profundus* in Whidden, 2000
13. *Pectoantebrachialis* (Figure 4)	Anterior part of manubrium (sternum)	Most distal part of deltopectoral crest, the pectoralis ridge (humerus)	Humeral abductor	
14. *Pectoralis major* (Figure 4)	Ventral surface from manubrium to xiphoid process (sternum)	Most proximal part of deltopectoral crest, the lateral lamina (humerus)	Humeral abductor	
15. *Pectoralis minor* (Figure 4)	Manubrium and firsts sternebrae, more dorsally than m. *pectoralis major* (sternum)	Most proximal part of deltopectoral crest, the lateral lamina (humerus)	Humeral abductor	
16. *Teres major* (Figures 3 and 4)	One tendon posterior to *supraspinous* fossa, and one tendon lateral to m. *subscapularis* origin (scapula)	Lateral border of *teres* tubercle (humerus)	Humeral abductor	
17. *Subscapularis* (Figures 3 and 4)	*Subscapularis* fossa (scapula)	Proximal end of lesser tubercle (humerus)	Humeral abductor	
18. *Cleidodeltoideus* (Figures 2 and 4)	Dorsally on the articular facet of the humero-clavicular joint (clavicle)	Lateral and medial border of deltoid fossa (humerus)	Humeral adductor, shoulder extensor	Considered as one muscle with m. *spinodeltoideus*, m. *deltoideus*, subdivided in three parts in Jullien, 1967; m. *deltoideus pars clavicularis* in Castiella et al., 1992
19. *Acromiodeltoideus* (Figures 2 and 4)	Dorsally on the articular facet of the humero-clavicular joint (clavicle)	Lateral and medial border of deltoid fossa (humerus)	Humeral adductor, shoulder extensor	
20. *Spinodeltoideus* (Figures 3 and 4)	Posterior part of the scapular spine (scapula)	Tip of the deltoid process (humerus)	Humeral adductor, shoulder flexor	m. *deltoideus pars scapularis* in Castiella et al., 1992
21. *Supraspinatus* (Figures 3 and 4)	Posterior part of supraspinous fossa (scapula)	Medial to humeral head, posterior to the greater tubercle (humerus)	Humeral adductor	
22. *Epitrochlearis*	Superficial sheet of m. *latissimus dorsi*	Olecranon, superficial to digital and carpal flexors (ulna)	Elbow extensor	m. *dorsoepitrochlearis* in Jullien, 1967; Castiella et al., 1992 and Whidden, 2000
23. *Triceps brachii caput longum* (Figures 3 and 5)	Lateral side of the scapular spine and acromion (scapula)	Dorsal part of the olecranon proximal crest (ulna)	Elbow extensor, shoulder flexor	m. *triceps brachii*, *caput longus* in Whidden, 2000
24. *Triceps brachii caput laterale* (Figures 4 and 5)	Anterior side of deltoid process (humerus)	Medial part of olecranon proximal crest (ulna)	Elbow extensor	m. *triceps brachii*, *caput lateralis* in Whidden, 2000
25. *Triceps brachii caput mediale* (Figures 4 and 5)	Anterior side of *teres* tubercle and posteriorly from beneath the bicipital canal to the brachialis fossa (humerus)	Lateral part of olecranon proximal crest (ulna)	Elbow extensor	m. *triceps brachii*, *caput medialis* in Whidden, 2000
26. *Anconeus* (Figures 4 and 5)	Posterior side of lateral epicondyle (humerus)	Medial part of olecranon proximal crest, more ventrally than m. *t.b. caput laterale* (ulna)	Elbow extensor	m. *anconeus pars lateralis* in Castiella et al.,1992; m. *anconeus lateralis* in Whidden, 2000
27. *Triceps brachii caput accessorium* (Figures 4 and 5)	Posterior side of medial epicondyle (humerus)	Lateral part of olecranon proximal crest, more distally than m. *t.b. caput mediale* (ulna)	Elbow extensor	m. *epitrochleo-anconeus* in Jullien, 1967 and Whidden, 2000; m. *anconeus pars medialis* in Castiella et al., 1992

(Continues)

TABLE 3 (Continued)

Muscle name	Origin	Insertion	Function.s	Remarks
28. *Biceps brachii* (Figures 3 and 6)	Tiny distal process near the glenoid cavity (scapula)	Medial side of the proximal half of the radius	Elbow flexor, humeral adductor	
29. *Pronator teres* (Figures 4 and 6)	Anterior side of medial epicondyle (humerus)	Ventral side of the radius, a bit more distally than m. *biceps brachii*	Elbow flexor	m. *pronator radii teres* in Whidden, 2000
30. *Brachialis* (Figures 4 and 5)	Brachialis fossa (humerus)	Ventrally, distal to the coronoid process (ulna)	Elbow flexor	m. *brachialis anticus* in Jullien, 1967 and Castiella et al., 1992
31. *Extensor carpi radialis* (Figures 4 and 7)	Medial part of lateral epicondyle (humerus)	Dorsally, on a proximomedial surface of 3rd metacarpal	Carpal extensor	
32. *Extensor digitorum lateralis* (Figures 4, 5 and 7)	Distal part of lateral epicondyle (humerus) and medial part of olecranon proximal crest (ulna)	Dorsally, on a distolateral surface of the middle phalanx of digit V	Carpal and digital extensor	m. *extensor digiti minimi* in Jullien, 1967 and Castiella et al., 1992; m. *extensor digiti quinti proprius* in Whalden, 2000
33. *Extensor digitorum communis* (Figures 4 and 7)	Proximal part of lateral epicondyle (humerus)	Sesamoid bones between proximal and middle phalanges of digits II, III, IV, and V	Carpal and digital extensor	
34. *Extensor digiti I and II* (Figures 5 and 7)	Medially, on the most proximal part of the posterior crest and the distal side of the proximal crest of olecranon (ulna)	Sesamoid bones, between proximal and middle phalanges of digit II and between 1st metacarpal and proximal phalanx of digit I	Carpal and digital extensor	m. *extensor indicis et pollicis longus* in Jullien, 1967; Castiella et al., 1992 and Whidden, 2000
35. *Abductor pollicis* (Figures 5, 6 and 7)	Distal to the proximal crest of olecranon on the dorsomedial side (ulna) and on the capitular process (radius)	Proximomedial surface of 1st metacarpal	Carpal extensor	m. *abductor pollicis longus* in Jullien, 1967; Castiella et al., 1992 and Whidden, 2000
36. *Flexor carpi ulnaris* (Figures 5 and 7)	Laterally, on the most proximal part of the posterior crest and the distal side of the proximal crest of olecranon (ulna)	Proximomedial surface of the pisiform	Carpal flexor	
37. *Flexor digitorum profundus* (Figures 4, 5 and 7)	Tendinous part from the cavity distal to the medial epicondyle (humerus), and muscular part from the lateral side of the posterior crest (ulna)	Proximal phalanges of the five digits, near the beginning of the claws	Digital flexor	
38. *Flexor digitorum superficialis* (Figures 4 and 7)	Distal part of medial epicondyle (humerus)	Distomedial surface of 2nd, 3rd and 4th metacarpals	Digital and carpal flexor	
39. *Palmaris longus* (Figures 4 and 7)	Proximal part of medial epicondyle (humerus)	Proximolateral surface of falciform bone and middle phalanx of digit V	Carpal flexor	

(Tables 2 and 3). Notes on muscle distinction and names given by previous authors are also provided when different. Muscle terminology was updated following Böhmer et al. (2021).

Most muscles inserting on the clavicle are described but were not considered for quantitative analyses as they did not have identified functions allowing forelimb movement. The m. *cleidodeltoideus* and m. *acromiodeltoideus* are small muscles described separately but were dissected together due to the difficulty of separation and similarity of their attachment sites and function. The m. *latissimus dorsi* and its superficial sheet, m. *latissimus dorsi superficialis* data were fused as they had similar length and orientation. Finally, a dataset of 34 muscles was used to perform our quantitative analyses.

To study functional variation at the inter and intraspecific levels, the muscles were classified into 14 functional groups based on Edwards (1937), Rose et al. (2013), Böhmer et al. (2021), and our observations. To define these functional groups, we considered movements of retraction/protraction of the scapula, movements of abduction/adduction of the scapula and humerus, which move the bones away from and toward the body axis, and the movements of flexion/extension at the shoulder, elbow, wrist, and digits. Some muscles were included in more than one functional group (Table 2).

2.2 | Muscles measurements

Muscles of the left forelimb were identified and detached individually from the point of origin to the point of insertion after removal of the skin and the fasciae. In case of damaged muscles, the right forelimb was dissected. Origin and insertion sites were recorded and each muscle was preserved in a 70% ethanol solution after being removed. Muscles were then blotted dry and weighed to the nearest 0.01 g using a Mettler AE100 Electronic balance. Next, muscles were transferred to a 30% nitric acid solution and left for approximately 24 h until the connective tissue was digested (Loeb & Gans, 1986). Once the fibres could be separated, the nitric acid was removed, and they were immersed in a 50% aqueous glycerol solution.

For each muscle, 10 fibres were randomly selected and fibre length was measured using, depending on their size, a digital caliper or a numeric measurement tool connected to a stereoscopic microscope for the smallest muscles, and a known scale. A mean fibre length for each muscle was then computed (in mm, Table S1). The volume of each muscle (in cm^3, Table S1) was calculated by dividing its mass (in g, Table S1) by muscle density (1.06 $g.cm^{-3}$; Mendez & Keys, 1960). PCSA (in cm^2, Table S1) was then calculated by dividing muscle volume by its mean fibre length (converted to cm). No correction for pennation angles was applied because pennation angles are known to be small in the forelimb muscles, thus having only a minor impact on the overall PCSA (Hartstone-Rose et al., 2012; Taverne et al., 2018). As notified by Rose et al. (2013), many of the mole's forelimb muscles have no internal tendons, fascicles spanning nearly the entire length of the muscle belly or are too small to measure this angle correctly. Furthermore, considering muscles for which Rose et al. (2013) performed a measure of the pennation angle in *Scalopus aquaticus*, our measures only differ very slightly. Muscle isometric force (F_{max}, in N; Table S1) was estimated by multiplying PCSA values by 30. This value corresponds to a maximum isometric stress of 30 $N.cm^{-2}$ and is applied following Woledge et al. (1985) and Medler (2002).

2.3 | Statistical analyses

We focused on three measures of interest for our analyses: muscle mass (MM), PCSA, and isometric force. For each measure, we designed two datasets, one with the values of each muscle separately and one with functional group variables that were designed by summing the values of all the individual muscles belonging to a given functional group. To describe quantitative muscle features we performed descriptive statistics on MM and estimated isometric force datasets. We then performed multivariate analyses on the PCSA datasets to study variations and covariations.

To describe MM distribution, as Rose et al. (2013) did for *S. aquaticus*, we first calculated the total weight of the forelimb, as the sum of all muscles, and secondly the percentage of the total weight represented by each muscle functional group. Average percentages were finally calculated for each functional group considering, in our calculation, *T. europaea* specimens only, then all the *T. aquitania* specimens, and finally *T. aquitania* specimens from Gironde and Aveyron separately. Histograms were used to represent the mass distribution based on these average percentages for the different species and populations. Isometric force distribution was also represented as histograms based on the average isometric force calculated for each functional group considering, as previously, *T. europaea* specimens only, all the *T. aquitania* specimens, and the *T. aquitania* specimens separated into two populations, from Gironde and Aveyron.

To analyse variation in the PCSA datasets, the measures of PCSA were $\log_{10}$ transformed to normalise and render them homoscedastic, and the effect of size was removed by regressing all variables against the total weight of the forelimb. Principal Component Analyses (PCA, *'prcomp'* function in 'stats' package in R; version 4.4.2, R Core Team, 2024) were performed on the resulting residuals of the regression to understand their distribution. The effect of allometry, defined as 'size-related changes in morphological traits' (Klingenberg, 2016), on PCA principal components was also tested using '*procD.lm*' function ('geomorph' package; Adams et al., 2021) which performs a Procustes ANOVA on the data. One general PCA was performed to quantify variation between all the functional groups. Further PCAs were performed to study variation within each of these groups. The data of all the individual muscles belonging to the given functional group were used to perform the latter. Biplots ('*biplot*' function in 'stats' package in R software), explaining the correlation of the variables with the axes of the PCAs were also generated.

Two other datasets were built with data obtained by Costes et al. (2023), who performed analyses of bone shape variation using 3D geometric morphometrics, one for the humerus and one for the ulna of moles. The superimposed 3D landmark coordinates of the nine specimens, used for the anatomical dissections, were extracted from their datasets and used to perform PCA and 3D visualisations of bone shape variation.

To analyse covariation of the muscle force with bone shape, we performed two-block partial least squares analysis (2BPLS, '*two.b.pls*' function in 'geomorph' package in R; Adams et al., 2021) considering PCSA and superimposed landmark coordinates datasets. We used the principal components of PCA representing 90% of the total variation of the superimposed landmark coordinates dataset and of each functional group PCSA datasets, as variables. The use of these principal components as variables allowed us to reduce data dimensionality as many statistical approaches can be sensitive to high dimensionality datasets (Baylac & Frieß, 2005). p-values were calculated based on 1000 permutations. We mainly investigated covariations of humerus and ulna shape with muscles involved in their movements or having at least an insertion site on one of the two bones. Thus, scapular abductors/adductors and protractors/retractors, were not included in these analyses.

To visualise shape variations of ulna and humerus depending on PCSA variations we used the '*shape. predictor*' function ('geomorph' package; Adams et al., 2021). This function allowed us to estimate shape deformations associated with minimum and maximum end of the first axis of the 2BPLS, based on one or more linear predictors, corresponding here to each functional group PCSA datasets. Then, we used '*tps3d*' ('Morpho' package; Schlager, 2017) and '*shade3d*' ('rgl' package; Murdoch & Adler, 2021) to draw 3D meshes of bone shape deformations.

3 | RESULTS

3.1 | Description of muscles architecture in *Talpa* species

We did not note any qualitative differences concerning the forelimb muscle architecture and insertion sites, neither between the two species nor between the two populations of *T. aquitania* (Gironde and Aveyron). Muscle names, insertion sites, and functions are provided in Table 3, with notes indicating differences with the work of previous authors. Observed muscle insertion sites are depicted on 3D meshes of the different forelimb bones in Figures 2–7. Pictures of the anatomical dissections depicting the muscular system are provided in Figures S2, S3, S4, and S5.

Talpa forelimb muscle masses range on average from 0.008 g to 1 g (Table S2) and muscle volumes from 0.007 to 1 cm^3 (Table S2). The m. *teres major* represents the largest forelimb muscle, with a measured mass around 1 g in each species and a muscle volume from approximately 0.9 to 1 cm^3. The mm. *pectorales* complex has a mass of around 0.95 g and a muscle volume around 0.9 cm^3. The m. *teres major* is also the muscle with the highest PCSA values of around 0.55 to 0.69 cm^2, which corresponds to an estimated isometric force-producing capacity of 16.6–20.6 N (Table S2). Therefore, this muscle produces almost half of the estimated isometric force of the humeral abductors (which range from approximately 44 to 49 N, Table S3). Muscle fibre length ranges from 3 to more than 40 mm (Table S2). The m. *latissimus dorsi* displays the greatest fibre length (measured length between 38 and 45 mm approximately), with fibres spanning nearly the entire length of the muscle (parallel fibre architecture). The smallest forelimb muscle is the m. *flexor digitorum superficialis*, which displays the lowest MM (0.008–0.009 g), the lowest muscle volume (0.007–0.008 cm^3) and the shortest fibre

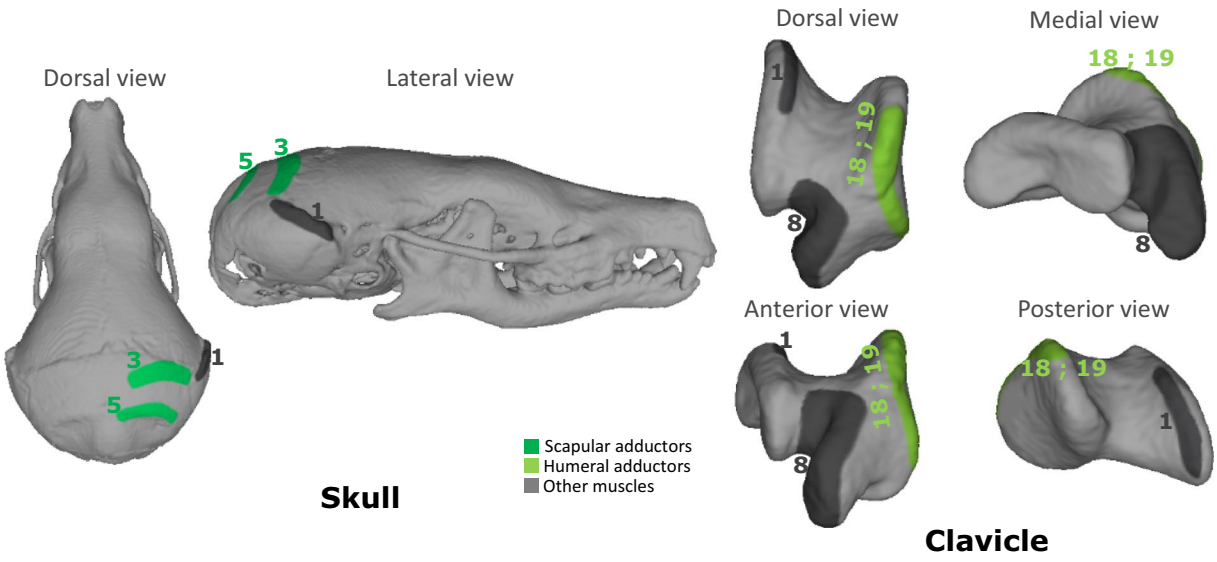

FIGURE 2 Muscle insertion sites of the skull and right clavicle of *T. aquitania*. Insertion sites correspond to coloured areas on the 3D meshes of each bone. Colours correspond to the functional groups identified in Table 2. Numbers associated with insertion sites correspond to muscle numbers in Table 3.

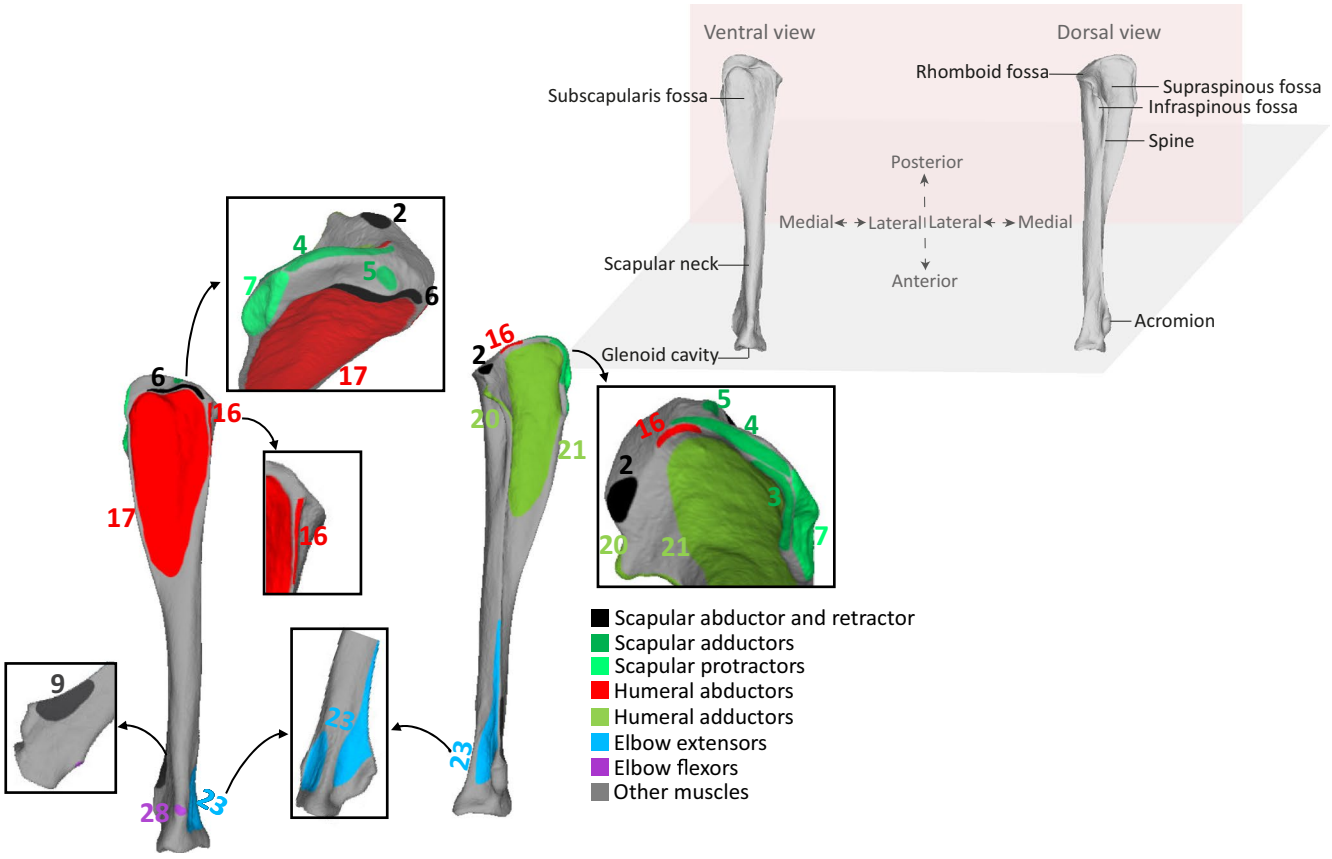

FIGURE 3 Anatomy and muscle insertion sites of the right scapula of *T. aquitania*. Names of anatomical parts are captioned and muscle insertion sites correspond to coloured areas on the 3D mesh of the bone. Colours correspond to the functional groups identified in Table 2. Numbers associated with insertion sites correspond to muscle numbers in Table 3.

lengths (2.8–3.6 mm). This muscle also has the lowest PCSA values (0.020 cm^2) in Gironde specimens of *T. aquitania*. In all the other specimen groups, the lowest PCSA values are found in the m. *spinotrapezius* (ranging from 0.016–0.021 cm^2).

3.2 | Functional distribution of forelimb muscle mass and isometric force in *Talpa* species

T. europaea and *T. aquitania* MM distribution according to the functional groups identified is following a proximal-to-distal reduction of MM considering the intrinsic muscles only (Figure 8). Humeral abductors represent the largest functional group and account for approximately 60% of the forelimb's total weight in the two species and in the two populations of *T. aquitania*. The elbow extensors are the second largest functional group, accounting for more than 12% of the forelimb's mass both in our inter and intraspecific groups.

In our analysis, we also considered extrinsic muscles as shoulder flexors/extensors and scapular muscles functional groups. Thus, we found the shoulder flexors as the third largest functional group, accounting for approximately 8%. In *T. aquitania*, the fourth largest functional group corresponds to scapular adductors accounting for approximately 6.5% of the forelimb's weight and the humeral adductors are only the fifth largest functional group. In *T. europaea* the humeral adductors are the fourth largest group. Accounting for approximately 6% of the forelimb's weight, the humeral adductors are very small compared with their antagonist muscle group, the humeral abductors (1/10th of their mass). The shoulder extensors are also very small compared with the shoulder flexors, as they account for less than 1% of the forelimb weight (approximately 1/9th of the flexors).

What is also noticeable is that carpal extensors are larger than the carpal flexors, and even than the elbow flexors in the Aveyron specimens of *T. aquitania*. The smallest muscle functional groups are the scapular retractors, shoulder extensors, carpal, and digital flexors.

Following MM functional distribution, the humeral abductors and the elbow extensors present the highest average estimated isometric force both at the inter and intraspecific level (respectively more than 40 N and around 20 N, Figure 9).

The same general functional distribution of average isometric force can be observed between the two species *T. europaea* and *T. aquitania* (Figure 9a and b). However, the humeral adductors now represent the third strongest group. They can produce, respectively, an average estimated isometric force of 10.5 N and 9.5 N in the two species which corresponds to approximately 1/4th of the estimated force produced by the antagonist humeral abductors. The shoulder flexors are the fourth strongest functional group, producing an

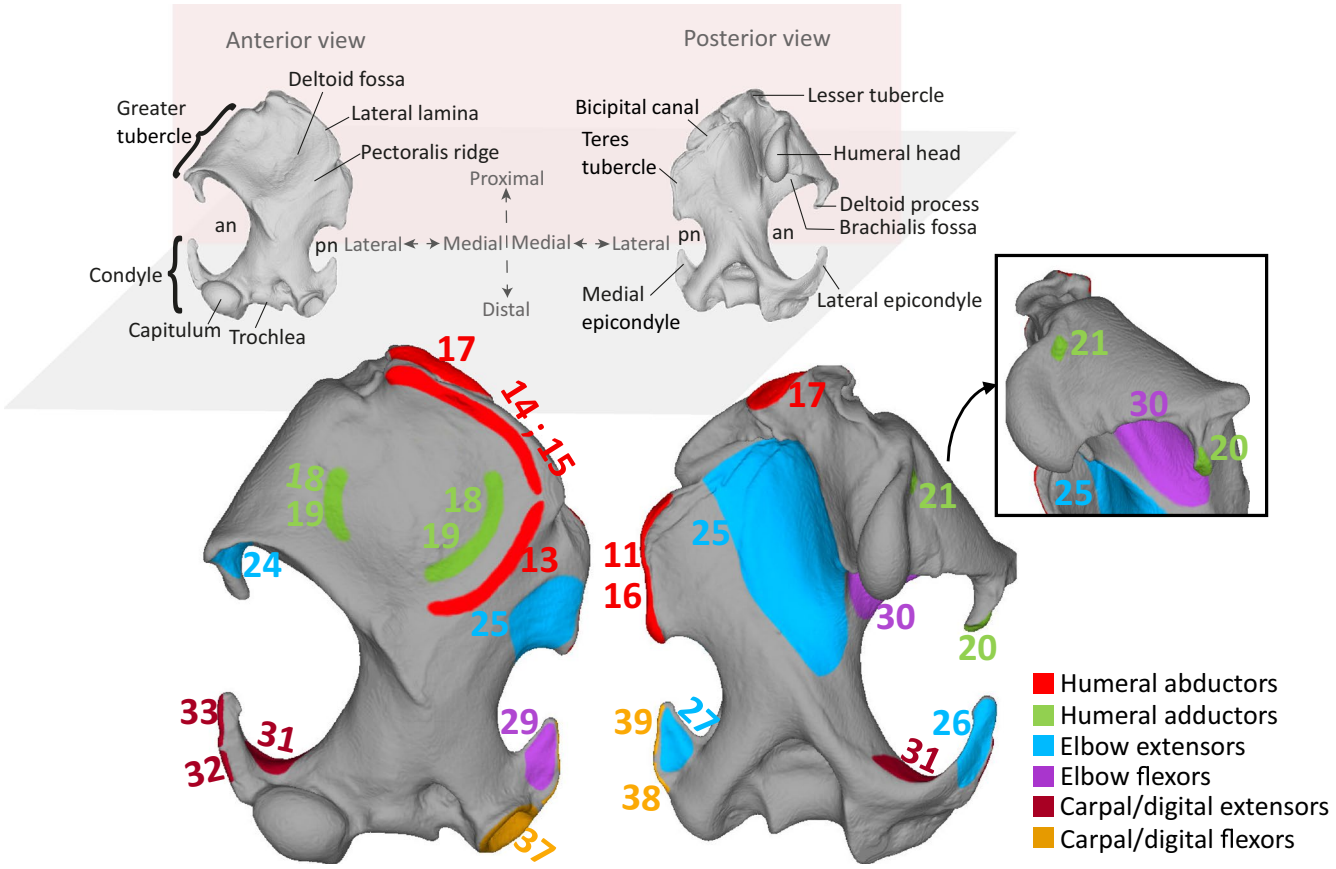

FIGURE 4 Anatomy and muscle insertion sites of the right humerus of *T. aquitania*. Names of anatomical parts are captioned and muscle insertion sites correspond to coloured areas on the 3D mesh of the bone. Colours correspond to the functional groups identified in Table 2. Numbers associated with insertion sites correspond to muscle numbers in Table 3. an: Anterior notch; pn: Posterior notch.

estimated isometric force of approximately 8.7 N in *T. europaea* and 9.5 N in *T. aquitania*. We can notice that the estimated force produced by their antagonist muscles, the shoulder extensors, is very small, representing only approximately 1/6th of the estimated force the flexors can generate. The elbow flexors represent the fifth largest group at the interspecific level, producing an estimated isometric force of 7.7–9.4 N, representing approximately half of the estimated force produced by the elbow extensors, their antagonist muscles.

At the intraspecific level, in *T. aquitania* specimens of Gironde and Aveyron, the humeral adductors are only the fourth largest functional group (Figure 9c and d). In Gironde specimens, the elbow flexors can produce a higher estimated isometric force compared with the humeral adductors (10.6 N compared with 9.4 N). In Aveyron specimens, the shoulder flexors are the third largest functional group before the humeral adductors (10.5 N compared with 9.7 N). Focusing on carpal/digital flexors and extensors, we can notice that the strongest group corresponds to the carpal extensors both at an inter and intraspecific level (producing an estimated isometric force from 6.7–7.7 N). Carpal flexors were one of the smallest functional groups considering MM distribution but not in terms of force production. They can produce a higher estimated isometric force than scapular abductors and retractors, shoulder extensors, and digital flexors in the two species and the two populations of *T. aquitania* (more than 3.5 N). In *T. europaea* they can also produce a higher estimated isometric force than scapular abductors and digital extensors. In *T. aquitania*, they can produce an isometric force that is similar to that of the digital extensors (approximately 3.7 N), which can even be slightly higher in Gironde specimens (3.58 N compared with 3.57 N).

3.3 | Inter and intraspecific variability of muscle force

The first two axes of the PCA (Figure 10) conducted on the PCSA dataset with the functional group variables represent 72.99% of the total variation (PC1: 45.57%; PC2: 27.42%). The Procrustes ANOVA performed on these two axes showed that there was no effect of allometry ($R^2 = 0$ and $p = 1$ for both axes) meaning that variation along these axes is not explained by size. The two species are separated along the second axis with *T. aquitania* at the maximum end of the axis and *T. europaea* at the minimum of the axis. The first axis separates the specimens of *T. aquitania* from Aveyron positioned toward the maximum of the axis and the specimens of *T. aquitania* from Gironde towards the minimum. *Talpa europaea* specimens are in an intermediate position along this axis. As shown by the length of their

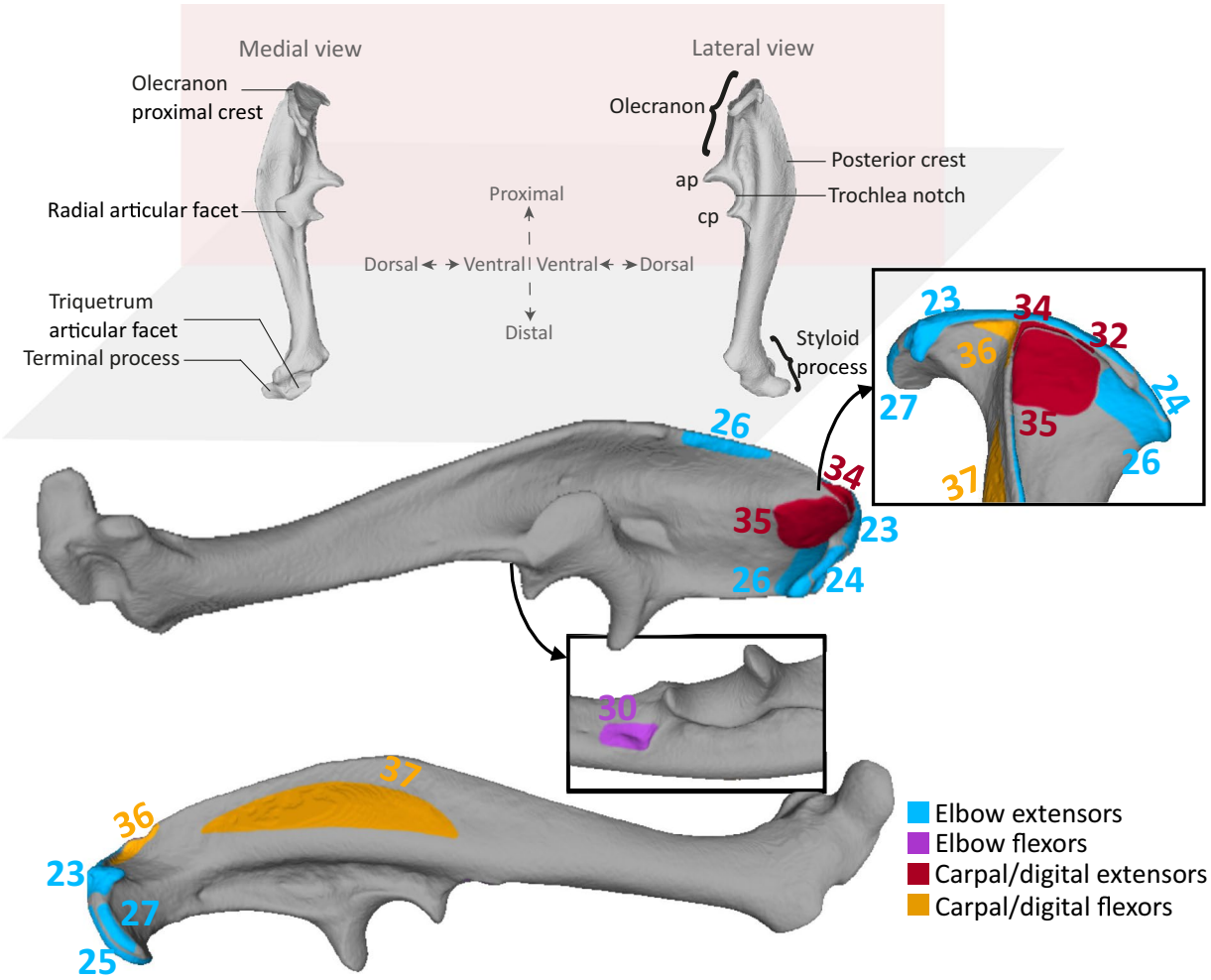

FIGURE 5 Anatomy and muscle insertion sites of the right ulna of *T. aquitania*. Names of anatomical parts are captioned and muscle insertion sites correspond to coloured areas on the 3D mesh of the bone. Colours correspond to the functional groups identified in Table 2. Numbers associated with insertion sites correspond to muscle numbers in Table 3.

vectors on the biplot, the variables explaining most the distribution of the specimens are the scapular adductors, scapular protractors, shoulder extensors, elbow flexors, carpal/digital flexors, and digital extensors. The scapular adductor vector is correlated to axis 2, showing that specimens at the maximum end of this axis (corresponding to *T. aquitania*) have higher PCSA values for these muscles than specimens at the minimum end (corresponding to *T. europaea*). The elbow flexor vector is opposed to shoulder extensors, humeral adductors, carpal, and digital flexors. The interspecific distribution is explained by this opposition: specimens at the maximum end of axis 2 (*T. aquitania*) have high PCSA values for the elbow flexors, while having small PCSA values for the humeral adductors, shoulder extensors, carpal, and digital flexors and conversely for the specimens at the minimum end (*T. europaea*).

The intraspecific distribution is mostly explained by scapular protractors, shoulder flexors, as well as carpal and digital extensors vectors. Specimens at the maximum end of axis 1 (specimens of *T. aquitania* from Aveyron) are thus associated with higher PCSA values for these muscles than specimens at the minimum end (specimens of *T. aquitania* from Gironde). The vector corresponding to the elbow flexors also partly explains this distribution. This vector shows that specimens of *T. aquitania* from the Gironde have higher PCSA values for elbow flexors compared with specimens from Aveyron.

The first two axes of the PCA conducted on the PCSA dataset of humeral abductors represent 84.36% of the total variation (PC1: 64.68%; PC2: 19.68%, Figure 11a). Concerning the humeral adductors, the first two axes of the associated PCA represent 95.66% of the total variation (PC1: 77.67%; PC2: 1799%, Figure 11b) and for the elbow extensors they represent 71.64% of the total variation (PC1: 45.66%; PC2: 25.98%, Figure 11c). The two species, *T. europaea* and *T. aquitania*, are only separated on two of the graphs, along the first axis of the humeral adductor PCA and along the second axis of the elbow extensor PCA. The two populations of Gironde and Aveyron of *T. aquitania* are separated on all the graphs, along the second axis for the humeral abductors and elbow extensors, and along the first axis for the humeral adductors. Here, the length of the vectors of the associated biplots show that the variables explaining best the distribution of the specimens for the humeral abductors are the m. *teres*

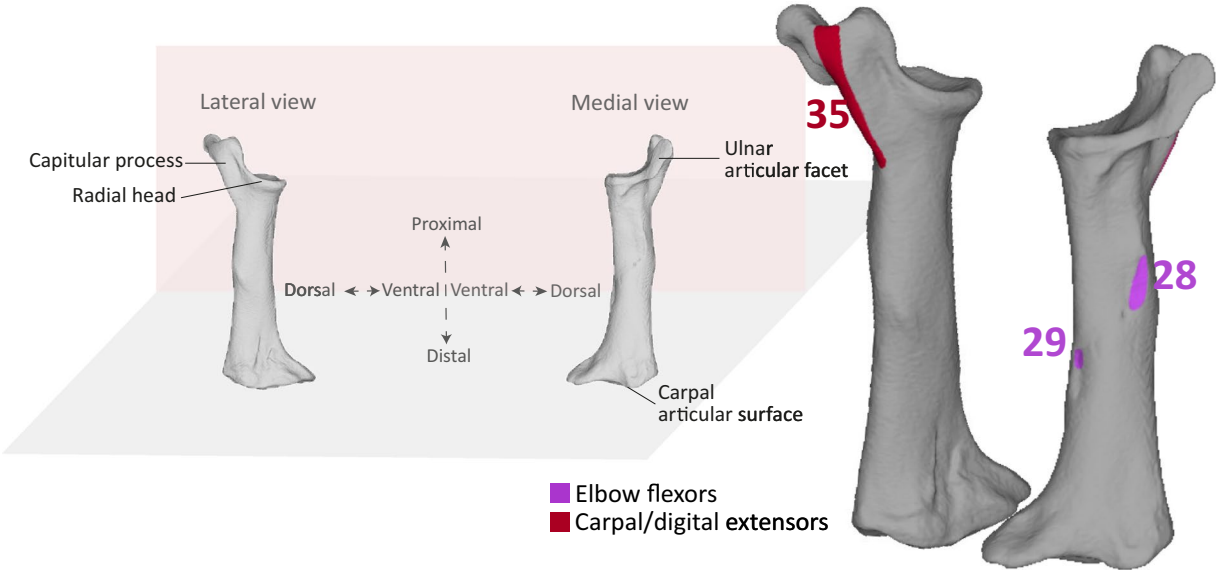

FIGURE 6 Anatomy and muscle insertion sites of the right radius of *T. aquitania*. Names of anatomical parts are captioned and muscle insertion sites correspond to coloured areas on the 3D mesh of the bone. Colours correspond to the functional groups identified in Table 2. Numbers associated with insertion sites correspond to muscle numbers in Table 3.

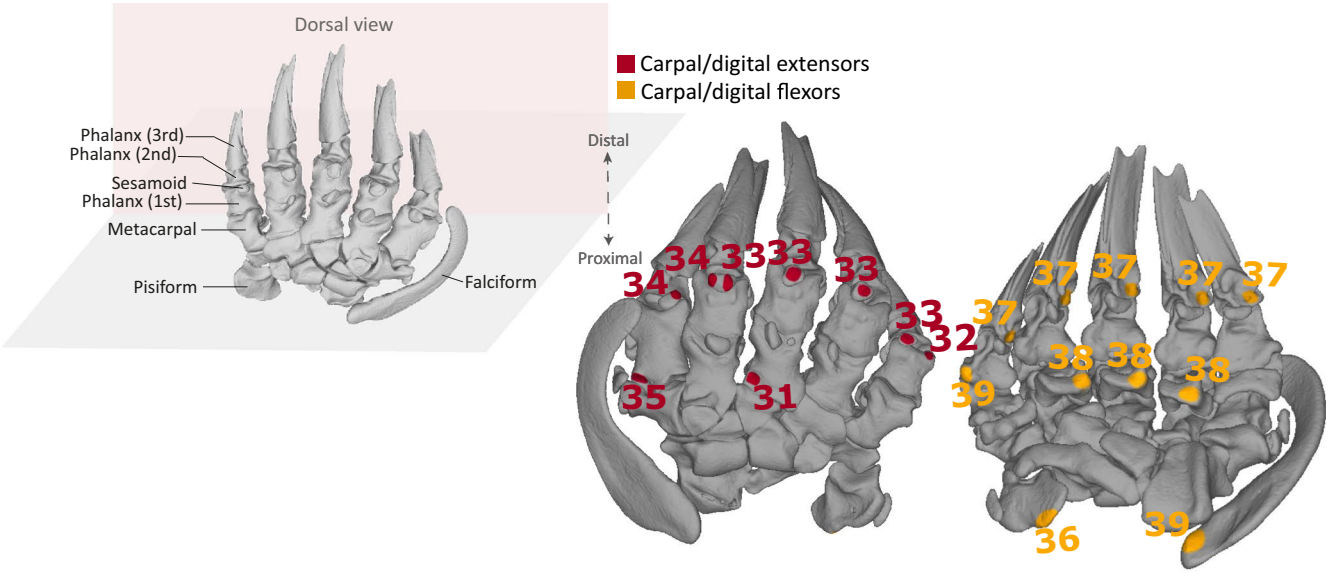

FIGURE 7 Anatomy and muscle insertion sites of the right manus of *T. aquitania*. Names of anatomical parts are captioned and muscle insertion sites correspond to coloured areas on the 3D mesh of the bone. Colours correspond to the functional groups identified in Table 2. Numbers associated with insertion sites correspond to muscle numbers in Table 3.

major (*T. minor* on the Figure 11a), the m. *pectoralis minor* (*P. minor*), the m. *pectoantebrachialis*, and the m. *pectoralis superficialis* (*P. superficialis*). For the humeral adductors, these variables correspond to the m. *cleidodeltoideus* and the m. *spinodeltoideus* and for the elbow extensors they correspond to the m. *triceps brachii caput longum* (*T. b. c. longum* on the Figure 11c), the m. *triceps brachii caput laterale* (*T. b. c. laterale*), and the m. *epitrochlearis*. The humeral abductors vectors mostly correlated with the second axis are the m. *pectoralis minor*, m. *teres major* and m. *pectoantebrachialis* which are opposed to the two other muscles vectors. Therefore, it explains the intraspecific distribution: specimens at the maximum of axis 2 (*T. aquitania* from Aveyron) have high PCSA values for m. *pectoralis minor* and m. *teres major* and small PCSA values for m. *pectoantebrachialis* and conversely for specimens at the minimum end of this axis (*T.aquitania* from Gironde and *T. europaea*). For the humeral adductors, m. *spinodeltoideus* and m. *supraspinatus* vectors are opposed to m. *biceps brachii* vector, and show that specimens at the maximum end of axis 1 (*T. europaea*) have high PCSA values for m. *spinodeltoideus* and m. *supraspinatus* while having small PCSA values for m. *biceps brachii* (*Biceps* on the Figure 11b), and conversely for specimens at the minimum end of this axis (*T. aquitania*

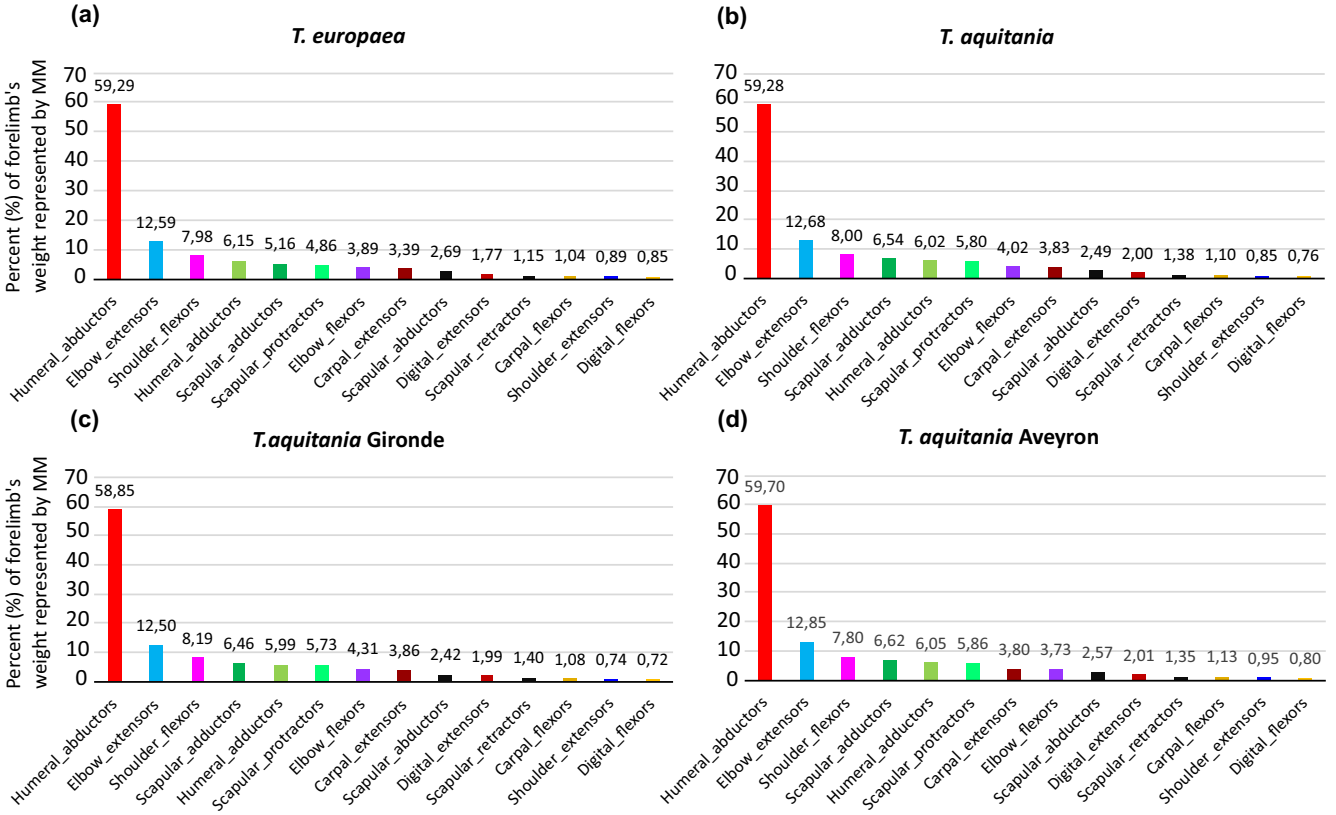

FIGURE 8 Functional muscle mass (MM, in g) distribution in *T. europaea* (a) and *T. aquitania* (b), and in *T. aquitania* populations of Gironde (c) and Aveyron (d). Each functional group mass corresponds to the sum of the individual muscle masses belonging to the given functional group and is expressed in percent (%) of the forelimb total weight. Average percentages, calculated for each species and each population, are depicted here.

and mostly specimens from Gironde). The m. *cleidodeltoideus* vector is associated with the second axis and does not explain the inter and intraspecific distribution of the specimens. For the elbow extensors, m. *triceps brachii caput longum* and m. *triceps brachii caput mediale* (*T. b. c. mediale* on the Figure 11c) vectors are opposed to m. *triceps brachii caput laterale* vector. As these vectors are mostly correlated with the second axis, they explain the inter and intraspecific distribution of the specimens: specimens at the maximum end of axis 2 (*T. europaea*) have high PCSA values for m. *triceps brachii caput laterale* and small PCSA values for m. *triceps brachii caput longum* and m. *triceps brachii caput mediale* and conversely for specimens at the minimum end of this axis (*T. aquitania*). As they group at the minimum end of the axis 2, specimens of *T. aquitania* from Aveyron have higher PCSA values for the m. *triceps brachii caput longum* and m. *triceps brachii caput mediale* and smaller PCSA values for the m. *triceps brachii caput laterale* than the specimens from Gironde.

3.4 | Covariations between bones shape and muscles force

PLS results (Table 4) show that the humerus and ulna are highly integrated ($r_{PLS}=0.966$) and that the covariation is significant ($p=0.032$) for the nine specimens of this study, as in Costes et al. (2023). Integration between humerus shape and PCSA variables is rather high (r_{PLS} always greater than 0.87) but is significant only between the bone shape and shoulder extensors ($p=0.008$), carpal/digital extensors ($p=0.003$ and 0.017 respectively) and carpal/digital flexors PCSA ($p=0.048$ and $p=0.038$ respectively). Considering the ulna, the only significant covariation is with the elbow extensors PCSA ($p=0.033$). Globally, the r_{PLS}, and thus the integration, is lower between ulna and PCSA variables. However, ulna shape is highly integrated with the elbow extensors PCSA ($r_{PLS}=0.954$).

The first axis of the PLS between humerus shape and shoulder extensor PCSA represents 100% of the total covariation (Figure 12). The two species as well as the two populations of *T. aquitania* are separated, with *T. europaea* being positioned towards maximum and Gironde specimens of *T. aquitania* towards the minimum; Aveyron specimens displaying a more intermediate position on the graph. Shoulder extensors insert on the deltoid fossa on the anterior side of the humerus. This area bulges more on the humerus shape associated with the minimum of the axis, thus with *T. aquitania* specimens. The shape associated with the maximum end of the axis, corresponding to *T. europaea* specimens, is associated with greater PCSA values for the shoulder extensors (Figure 10) and the deltoid fossa seems deeper, more concave.

Concerning the ulna shape and elbow extensor PCSA, the first axis of the PLS represents 63.6% of the total covariation

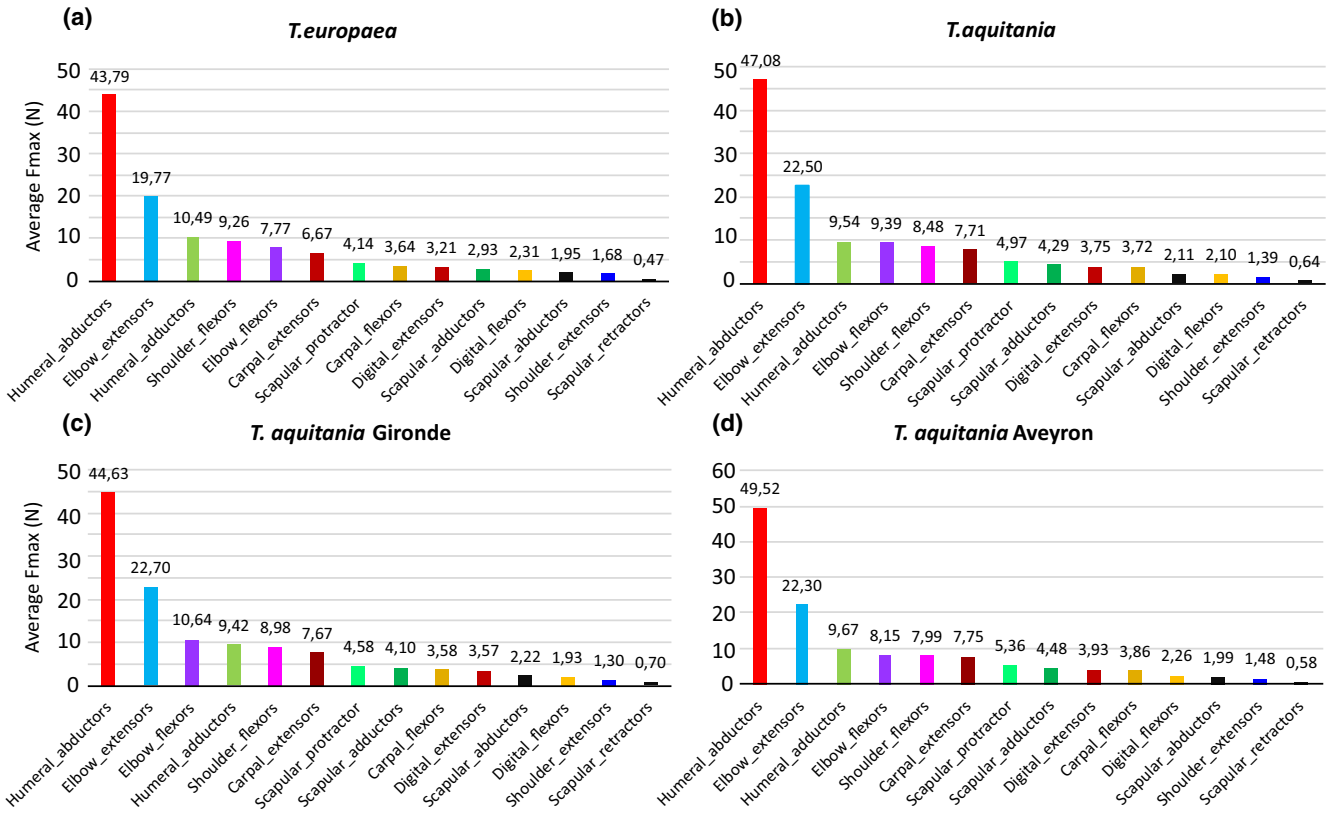

FIGURE 9 Functional isometric force (F_{max}, in N) distribution in *T. europaea* (a) and *T. aquitania* (b), and in *T. aquitania* populations of Gironde (c) and Aveyron (d). Each functional group estimation of isometric force was calculated as the sum of the individual muscle isometric forces belonging to the given functional group. Average isometric forces, calculated for each species and each population, are depicted here.

(Figure 13). As for the humerus shape and shoulder extensors, the two species and the two populations of *T. aquitania* are separated along this axis. *T. europaea* borders the axis on its maximum end, while Aveyron specimens of *T. aquitania* are positioned towards the minimum, and Gironde specimens are in an intermediate position. Elbow extensors are muscles inserting on the proximal crest of the ulna principally. Here shape covariation patterns show that specimens of *T. europaea* have a larger olecranon on the medial side (where the m. *triceps brachii caput laterale* and m. *anconeus* insert), whereas *T. aquitania* specimens, especially the Aveyron population, display a larger olecranon on the lateral side (where the m. *triceps brachii caput mediale* and m. *triceps brachii caput accessorium* insert). This is congruent with the results of the PCA on the elbow extensors dataset which showed that specimens of *T. aquitania*, especially in Aveyron, have greater PCSA values for the m. *triceps brachii caput longum* and m. *triceps brachii caput mediale*, while *T. europaea* specimens have greater PCSA values for the m. *triceps brachii caput laterale*.

Concerning the significant covariation of humerus shape with carpal/digital extensors and carpal/digital flexors PCSA, no inter and intraspecific structuring can be seen along the first axis of the PLS on the graphs (Figure S1). Specimen discrimination at the inter and intraspecific level can, however, be noticed along the second axis of the PLS for the carpal and digital extensors (Figure 14). This axis represents, respectively, 33.4% and 31.9% of the total covariation of each PLS.

4 | DISCUSSION

In this study we provide descriptions of the forelimb musculature of two *Talpa* species, including the recently described *T. aquitania*. We found no qualitative differences to distinguish *T. europaea* from *T. aquitania* based on the musculature, but we highlight quantitative differences between the two species, especially in muscle PCSA and thus in force-producing capacity. Variations in muscle PCSA were also observed at an intraspecific level between the two populations of *T. aquitania*.

4.1 | Forelimb musculature of *Talpa* species

In accordance with the literature, we described 39 extrinsic and intrinsic forelimb muscles. Therefore, only 36 muscles which generate forces that move the scapula, humerus, ulna, radius, and the manus were considered as involved in forelimb motion during digging. The m. *cleidomastoideus* (as described in Jullien, 1967; Castiella et al., 1992; and Whidden, 2000, in *Talpa* species) was considered as

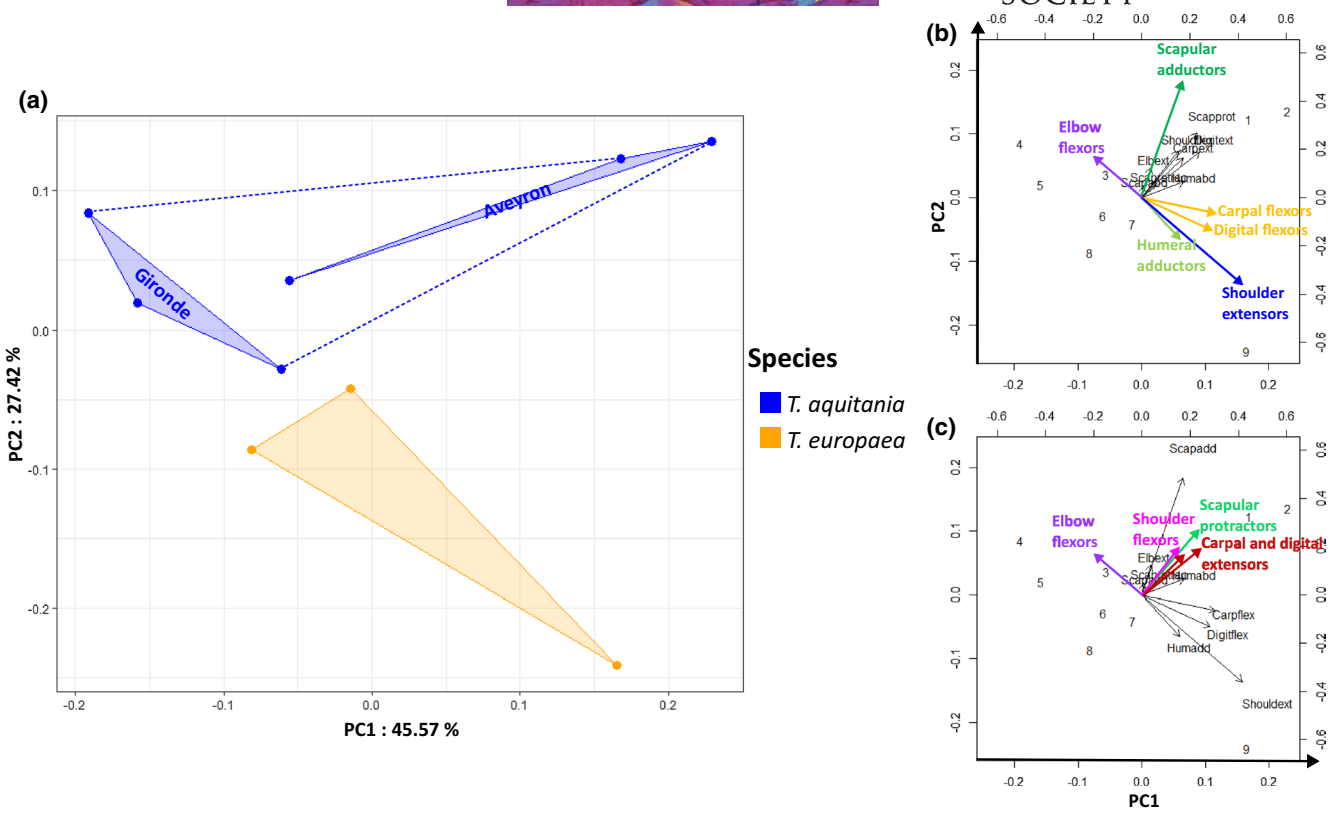

FIGURE 10 Graphic representation of the first two principal components (PCs) of the PCA performed on the PCSA general dataset (a). Each specimen, represented by a point, was coloured according to its species. The two populations of *T. aquitania* from Aveyron and Gironde are separated in two groups on the graphs with pointed lines delimitating the species. The associated biplot, which allows to understand variables (i.e. muscle functional groups) correlation with the first two PCs of the PCA, can be seen on the right. Coloured vectors correspond to the variables mostly associated with PC2 (b) and PC1 (c).

involved in neck motion. For our analyses, we also did not consider the two small muscles moving the clavicle, the mm. *subclavius pars clavicularis* and *subclavius pars scapularis* as we were not able to collect sufficient data.

Most of the muscles we described were named following Böhmer et al. (2021) nomenclature to update and harmonise the terminology. Indeed, some muscles were given different names by the different authors that previously worked on the forelimb in *Talpa* species (Castiella et al., 1992; Jullien, 1967; Whidden, 2000). Some muscles were also divided and described differently. This is particularly true for the muscles inserting on the clavicle and the mm. *pectorales*. We had difficulty in individualising their different parts, as clavicle muscles are particularly small and pectoral muscles form a muscle complex.

Considering the mm. *pectorales*, Jullien (1967), only divided this muscle into two parts, the m. *pectoralis major* and the m. *pectoralis minor*, with one bundle of its m. *pectoralis major* corresponding to the m. *pectoantebrachialis* we individualised. In Castiella et al. (1992), both our m. *pectoantebrachialis* and m. *pectoralis major* were divided into two different parts, leading the authors to recognise five parts in the pectoral complex. Whidden (2000) described four parts in this complex, dividing what we called the m. *pectoralis major* into two different parts, the m. *pectoralis superficialis pars posticus* and the m. *pectoralis abdominalis*. Paying particular attention to these different descriptions, we described four parts in the mm. *pectorales*, including a superficial sheet inserting into the integument we named the m. *pectoralis superficialis*, but also the m. *pectoantebrachialis*, the m. *pectoralis major*, and the m. *pectoralis minor*.

Differences were also found in the description of muscles inserting on the clavicle. Especially, the m. *cleidodeltoideus* and the m. *acromiodeltoideus* were considered as one muscle, the m. *deltoideus pars clavicularis*, in Castiella et al. (1992), but were separated for all the other authors and according to our observations. Castiella et al. (1992) also described four small muscles inserting between the sternum and the clavicle and/or the scapula, the m. *subclavius*, the m. *costoscapularis pars dorsalis*, the m. *costoscapularis pars ventralis*, and the m. *sternoclavicularis*. Jullien (1967) only described the m. *subclavius* and the m. *costoscapularis* that he divided into two bundles, and Whidden (2000) considered only one muscle, the m. *subclavius* that he divided into three bundles. Here we only found the m. *subclavius* that we divided into two parts: the m. *subclavis pars clavicularis*, and the m. *subclavius pars scapularis*.

The *rhomboideus* muscles have also received special attention, resulting in differences between our observations and descriptions of the insertion sites in previous studies. Indeed, we found the m. *rhomboideus profundus* origin near the parieto-occipital suture,

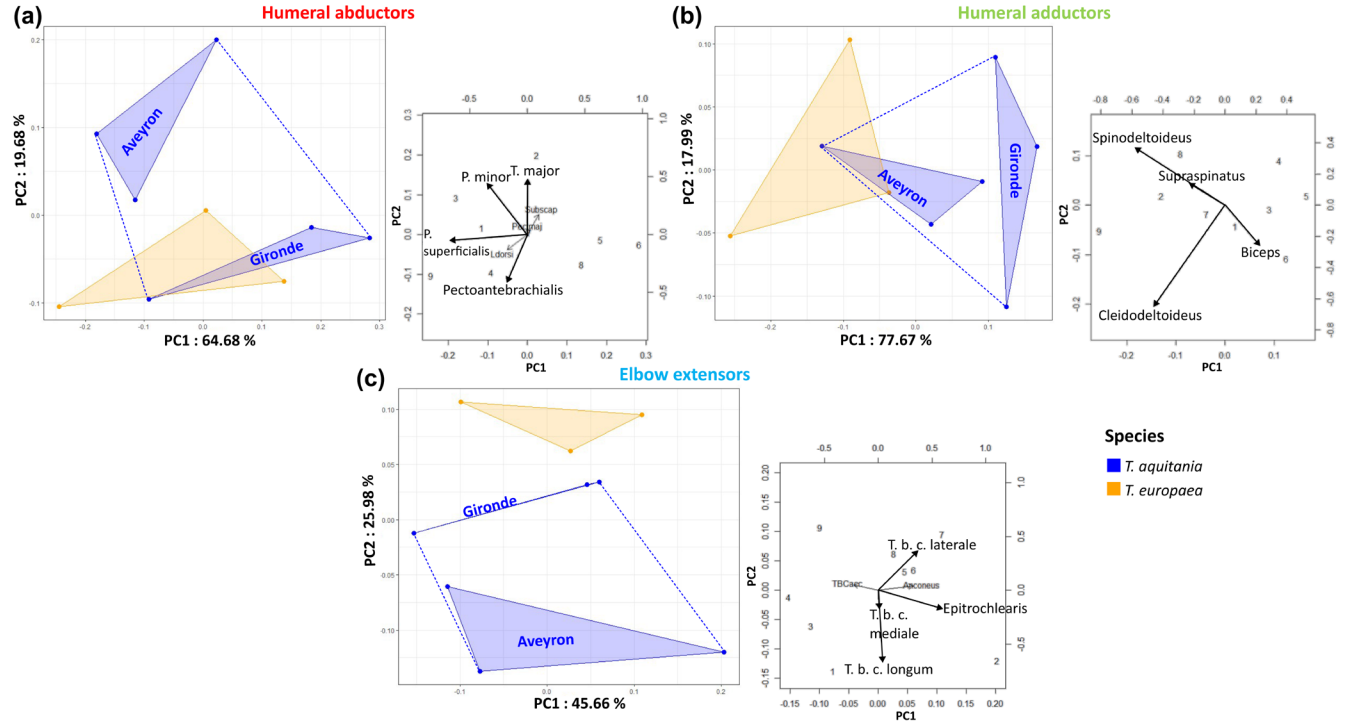

FIGURE 11 Graphic representation of the first two principal components (PCs) of the PCAs performed on the PCSA datasets of the humeral abductors (a), the humeral adductors (b) and the elbow extensors (c). Each specimen, represented by a point, was coloured according to its species. The two populations of *T. aquitania* from Aveyron and Gironde are separated in two groups on the graphs with pointed lines delimitating the species. The associated biplots, which allow to understand variables (i.e. individual muscles belonging to each functional groups) correlation with the first two PCs of the PCAs, are also shown. *P. minor*: *Pectoralis minor*; *P. superficialis*: *Pectoralis superficialis*; *T. major*: *Teres major*; *T. b. c. laterale*: *Triceps brachii caput laterale*; *T. b. c. longum*: *Triceps brachii caput longum*; *T. b. c. mediale*: *Triceps brachii caput mediale*.

when previous authors found it on cervical (Whidden, 2000) or dorsal (Castiella et al., 1992; Jullien, 1967) vertebral processes. This muscle was particularly easy to identify by the interscapular ligament that extends it to the scapula where it inserts. Castiella et al. (1992) described the m. *rhomboideus cervicis* as originating near the parieto-occipital suture, but consistent with Jullien (1967) and Whidden (2000) we found its origin on spinous processes of cervical vertebrae (they both described its origin as being on the nuchal ligament, and Jullien (1967) also found an insertion site on spinous processes of dorsal vertebrae).

As in Castiella et al., 1992 we did not find the m. *supinator* described in Jullien (1967) and Whidden (2000). We also did not find the m. *extensor carpi ulnaris* and m. *flexor carpi radialis* described in Whidden (2000) only. These two muscles of the forearm are, nonetheless, present in another fully fossorial mole from North-America, *S. aquaticus*, according to Edwards (1937) and Rose et al. (2013). Indeed, despite their similar locomotor habits, *Talpa* and *Scalopus* species display some muscular differences and other muscles as the m. *teres minor* and the m. *infraspinatus*, two humeral abductors, are present in *S. aquaticus* but absent in *T. europaea* and *T. aquitania*. On the contrary, the m. *spinodeltoideus* is reported present in *Talpa* species but not in *S. aquaticus*. Compared with other insectivores or non-fossorial Talpidae, studied respectively by Jullien (1967) and Whidden (2000), fully fossorial moles as *Talpa* or *Scalopus* species have lost some muscles of the shoulder including the m. *atlantoscapularis* or the *coracobrachialis*. Some other shoulder muscles are reduced such as the anterior trapezius muscle, whose presence is limited to only a few fibres. As for the other Talpidae, there is also a loss of the intrinsic muscles of the manus in these two genera, which are reported present by Jullien (1967) in other insectivorous species.

The forelimb musculature of the two *Talpa* species studied here, *T. europaea* and *T. aquitania*, is characterised by large humeral abductors and elbow extensors. Indeed, these two muscle groups are both the largest in terms of MM and the strongest considering the force-producing capacity (estimated by F_{max} values). The two more massive, stronger, and voluminous muscles in the forelimb correspond to two humeral abductors, the m. *teres major* and the mm. *pectorales*, when considered as a muscle complex. In both species, the two shoulder flexors (m. *spinodeltoideus* and m. *triceps brachii longum*) and the humeral adductors are also rather large and strong muscle groups. In terms of MM, the scapular adductors are also one of the largest groups but they display relatively low values for force-producing capacity, especially in *T. europaea*. On the contrary, elbow flexors are much less massive but they have a relatively high estimated force-producing capacity (being equivalent to those of the humeral adductors and the shoulder flexors in *T. aquitania*). Carpal extensors also display a high estimated force-producing capacity in comparison to their mass.

TABLE 4 Results of the covariations analyses (2BPLS) performed between humerus and ulna shape and muscle PCSA. r-PLS and *p-values* were obtained from the 2BPLS analyses performed on the principal components of the PCAs representing 90% of the variability of the two bones superimposed landmark coordinates datasets and 90% of the variability of each muscle functional group PCSA datasets.

		Humerus	Ulna
Humerus/Ulna	r_{PLS}	**0.966**	
	p-value	**0.032**	
Shoulder extensors	r_{PLS}	**0.969**	0.807
	p-value	**0.008**	0.356
Shoulder flexors	r_{PLS}	0.927	0.851
	p-value	0.105	0.23
Humeral abductors	r_{PLS}	0.909	0.761
	p-value	0.188	0.663
Humeral adductors	r_{PLS}	0.927	0.838
	p-value	0.115	0.265
Elbow extensors	r_{PLS}	0.892	**0.954**
	p-value	0.423	**0.033**
Elbow flexors	r_{PLS}	0.874	0.741
	p-value	0.403	0.704
Digital extensors	r_{PLS}	**0.965**	0.748
	p-value	**0.017**	0.67
Carpal extensors	r_{PLS}	**0.979**	0.727
	p-value	**0.003**	0.734
Digital flexors	r_{PLS}	**0.952**	0.832
	p-value	**0.038**	0.285
Carpal flexors	r_{PLS}	**0.948**	0.844
	p-value	**0.048**	0.268

Note: Significant results are in bold.

Focusing on intrinsic muscles (i.e. the humeral abductors and adductors, the elbow and carpal/digital flexors/extensors), we can notice a proximal-to-distal reduction patterns in muscles features (mass, volume, fibre length, and force-producing capacity), with muscles of the forearm (mostly carpal/digital flexors and extensors) representing most of the smallest and weakest muscles. It is also noticeable that antagonist muscle groups often display great differences in muscle architecture. Globally, the shoulder flexors, the scapular adductors and protractors, the humeral abductors, the elbow extensors, and the carpal/digital extensors are more massive and stronger than their antagonist muscles.

4.2 | Interspecific functional distribution of muscle mass and isometric force

Talpa europaea and *T. aquitania* show similar functional mass distributions. The only difference being for the scapular adductors which are larger than humeral adductors in *T. aquitania* (6.54% of total forelimb's weight) but not in *T. europaea* (5.16% of forelimb's weight). Despite similar distribution of MM, more differences can be noticed in estimated isometric force mean values (scapular adductors, humeral abductors, elbow flexors and extensors, and carpal extensors which have higher values in *T. aquitania*). No conclusion on interspecific variations can be made based on these values, as they were not scaled on the specimen size and *T. aquitania* is known to be the larger species, on average (Nicolas et al. reported, in 2017, an average weight of 89 ± 17 g in *T. Aquitania* significantly greater to the average weight of 76 ± 12 g in *T. europaea*). Nevertheless, we can notice that the functional distribution of the isometric force is also quite similar in the two species, except for the scapular adductors which have a reduced force-producing capacity compared with the carpal flexors and digital extensors in *T. europaea* (2.93 N) but not in *T. aquitania* (4.29 N). Our MM quantification is rather consistent with data from Gambaryan et al. (2002) and Rose et al. (2013) for respectively *T. europaea* and *S. aquaticus*.

The overall forelimb muscles patterns we described in *T. europaea* and *T. aquitania* are also consistent with what Rose et al. (2013) described in *S. aquaticus*. The proximal-to-distal reduction of intrinsic forelimb muscles has already been noticed by these authors, even if they did not include extrinsic muscles which move the scapula. We noticed that by adding scapular muscles to our analyses, the reduction of muscles features is no longer following this proximal-to-distal reduction in the two *Talpa* species as some of these muscles inserting proximally (scapular retractors, abductors and shoulder extensors) are part of the smallest and weakest muscles groups. On the contrary, considering MM, shoulder flexors appear as the third largest group (which corresponds to the humeral adductors, accounting for more than 8% of the forelimb's total weight in *S. aquaticus* according to Rose et al., 2013) and as the fourth strongest group considering the isometric force.

The humeral abductors, being the largest functional group in fully fossorial moles, represent around 60% of the total forelimb weight in *T. europaea* and *T. aquitania* (65% for *T. europaea* according to Gambaryan et al., 2002), a value closer to that found for *Scapanus*, another genus of North-American moles, by Reed in 1951 (55%) than to the value of Rose et al. (2013) for *S. aquaticus* (75%). These results can be related to the presence of the m. *teres minor* and m. *infraspinatus*, the additional humeral abductors described in *S. aquaticus*. Another difference with Rose et al. (2013) is that we found carpal/digital extensors that are larger and stronger than the carpal/digital flexors. This difference is probably mainly due to the m. *palmaris longus*, a carpal flexor situated in the forearm, which is one of the smallest muscles in *T. europaea* and *T. aquitania* forelimb according to our results (generating an isometric force between approximately 0.9 and 1.1 N and weighting 0.014 to 0.017 g in average, representing around 0.30% of the total weight of the forelimb, Table S2) and consistent with the values reported by Gambaryan et al. in 2002 (0.12% of the total weight of the forelimb). On the contrary, Rose et al. (2013) in *S. aquaticus* found an average isometric force of 7.1 N for this muscle and an average weight of 0.18 g, contributing to the major part of the 5% of the total weight of the forelimb represented

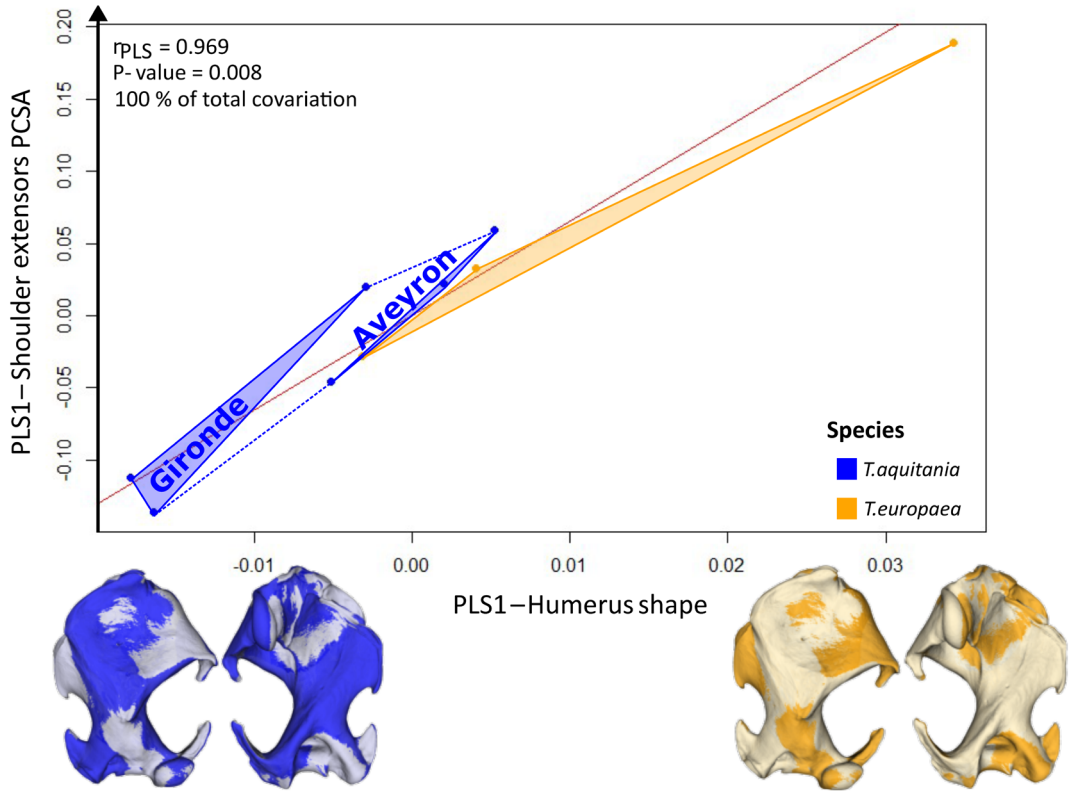

FIGURE 12 Graphic representation of the first axis of the two blocks partial least square (2BPLS) analysis performed between humerus shape data and shoulder extensors PCSA. The 2BPLS analysis was performed on the principal components of the PCA representing 90% of the total variation of the shoulder extensors PCSA dataset (plotted on the Y axis) and of the superimposed landmark coordinates dataset carrying shape information of the humerus (plotted on the X axis). Each specimen, represented by a point, was coloured according to its species. The two populations of *T. aquitania* from Aveyron and Gironde are separated in two groups on the graph with pointed lines delimitating the species. Shape variation associated with each extreme of the first PLS axis are represented: In blue shape associated with the minimum and in orange shape associated with the maximum of the axis. The mean shape, calculated as the mean of superimposed landmark coordinates, is superimposed, in clear grey, to each of these shapes to highlight shape variation.

by the carpal flexors, making it the largest muscles of the forearm in their study. According to our results, in *T. europaea* and *T. aquitania*, the largest muscle of the forearm corresponds to the m. *biceps brachii* (around 0.05–0.06 g in average, Table S2), and the carpal flexors represent no more than 1% of the total weight of the forelimb.

If MM distribution follows that of *S. aquaticus*, the isometric force distribution we found for *T. europaea* and *T. aquitania* is less consistent than reported in Rose et al. (2013). Indeed, in addition to the carpal flexors being stronger than the carpal extensors, the humeral adductors can produce a higher isometric force than the elbow extensors according to Rose and co-authors, whereas it is the opposite for the two *Talpa* species. Moreover, estimated isometric force-producing capacity is higher in the humeral abductors/adductors and lower in elbow extensors in *S. aquaticus* compared with *T. europaea* and *T. aquitania*. However, this can be due to size differences between species. Alternatively, these differences might be the marker of functional differences or can also be explained by preservation conditions of the specimens used. Indeed, we used specimens preserved in ethanol, while Rose et al. (2013) used frozen specimens. Martin et al. (2020) insist that all specimens used within a study have to be preserved in the same manner to ensure that potential decrease in mass and length is similar across all muscles. This may explain part of the observed differences; nevertheless, we noticed that even with correction factors, as those proposed by Leonard et al. (2022), the differences between our two studies for MM and isometric force values are not reduced.

4.3 | Functional description of mole forelimb

For our analyses, forelimb muscles were assigned to 14 different functional groups based on the movements they induce. At the shoulder joint, we considered movements of flexion/extension and movements allowing abduction/adduction (moving the bones away or toward the body midline) of both the scapula and the humerus. Scapular protractors/retractor muscles moving the bone forward (anteriorly) and backward (posteriorly) were also identified. At the elbow and carpal joints, we only considered movements of flexion/extension. We did not take into account movements in the transversal plane as rotation of bones, whereas rotation of the humerus around its longitudinal axis is possible as noted by Yalden (1966) and demonstrated by Gambaryan et al. (2002). Following Rose

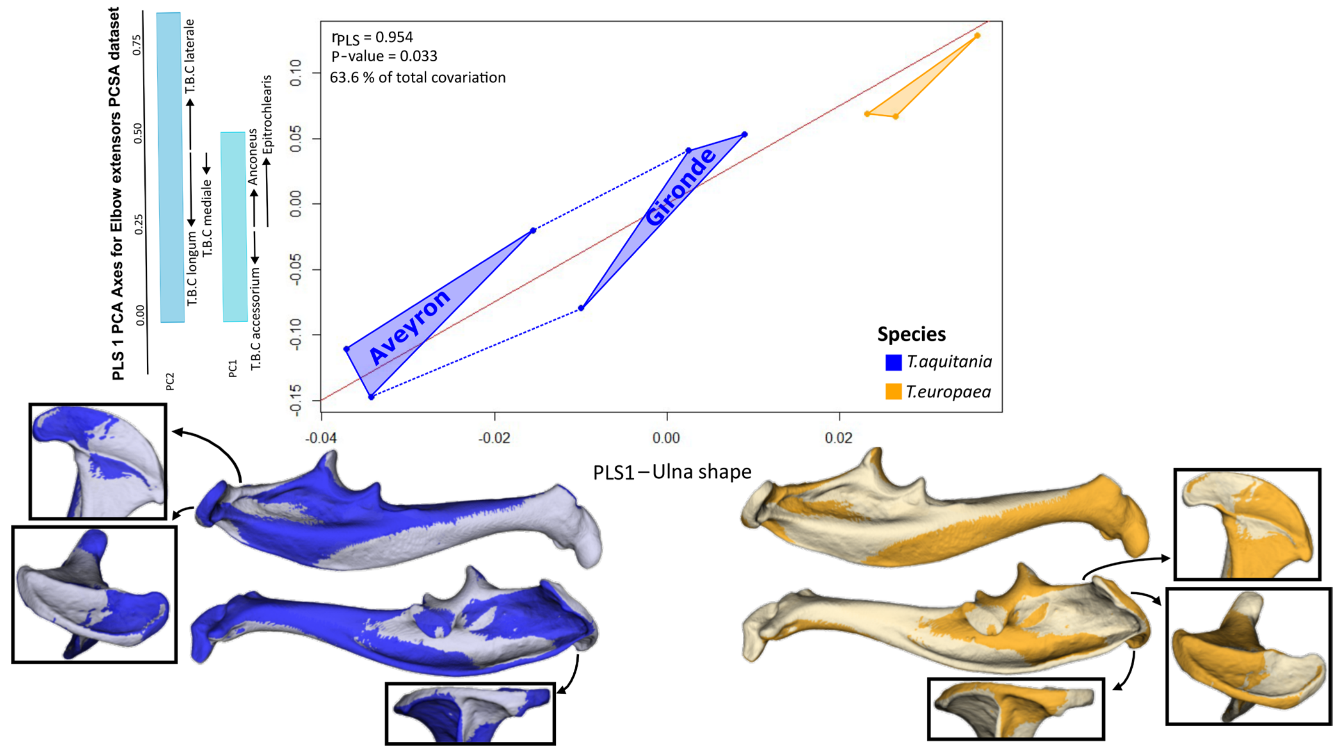

FIGURE 13 Graphic representation of the first axis of the two blocks partial least square (2BPLS) analysis performed between ulna shape data and elbow extensors PCSA. The 2BPLS analysis was performed on the principal components of the PCA representing 90% of the total variation of the elbow extensors PCSA dataset (plotted on the Y axis) and of the superimposed landmark coordinates dataset carrying shape information of the ulna (plotted on the X axis). Each specimen, represented by a point, was coloured according to its species. The two populations of *T. aquitania* from Aveyron and Gironde are separated in two groups on the graph with pointed lines delimitating the species. Shape variation associated with each extreme of the first PLS y axis are represented: In blue shape associated with the minimum and in orange shape associated with the maximum of the axis. The mean shape, calculated as the mean of superimposed landmark coordinates, is superimposed, in clear grey, to each of these shapes to highlight shape variation. PCA axes correlating the most with the x axis are also provided, with arrows representing variables that correlate the most with each PCA axes and indicating their orientation according to these axes. T.B.C.: Triceps brachii caput.

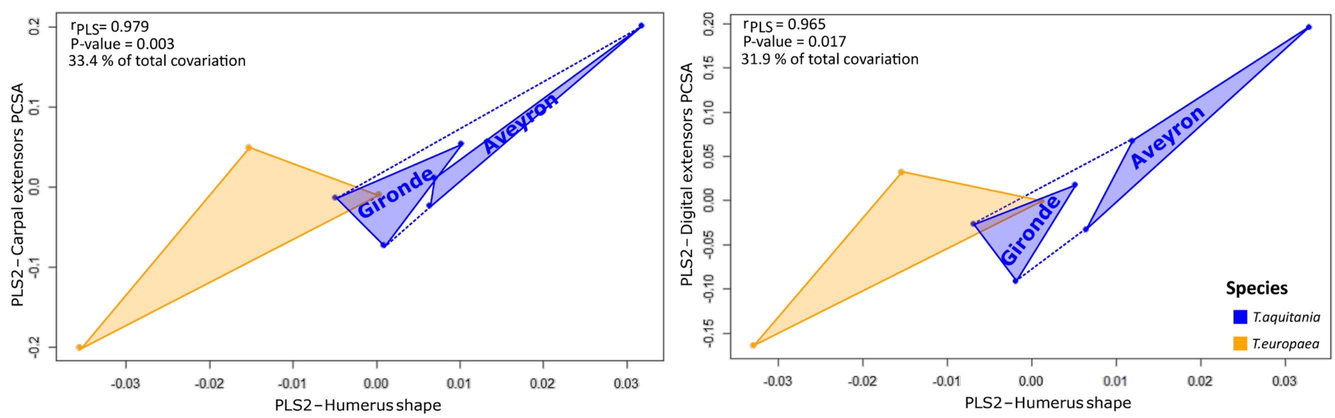

FIGURE 14 Graphic representations of the second axis of the two blocks partial least square (2BPLS) analyses performed between humerus shape data and carpal and digital extensors PCSA. The 2BPLS analyses were performed on the principal components of the PCA representing 90% of the total variation of the carpal and digital extensors PCSA datasets (both plotted on the Y axis) and of the superimposed landmark coordinates dataset carrying shape information of the humerus (plotted on the X axis). Each specimen, represented by a point, was coloured according to its species. The two populations of *T. aquitania* from Aveyron and Gironde are separated in two groups on the graphs with pointed lines delimitating the species.

et al. (2013), this longitudinal rotation of the humerus is mainly performed by the same muscles that allow humeral abduction. Supination and pronation movements were also not considered, as moles are known to be incapable of these movements at the carpal joint (Jullien, 1967; Yalden, 1966).

At the shoulder joint we can notice the elliptical, and not spherical, surface of the humeral head, allowing to move the humerus in two planes only. Gambaryan et al. (2002) already noticed that, compared with other mammals, the possible movements at the shoulder joint were reduced in moles and that abduction of the forelimb took place in the sternoclavicular joint rather than at the shoulder joint. This is consistent with the absence or reduction of some scapular/shoulder muscles in fully fossorial moles compared with other Talpidae or insectivores (Jullien, 1967; Whidden, 2000). Moreover, our results show that scapular adductors, that maintain the scapula towards body midline, generate higher isometric force than scapular abductors, which are represented by only one muscle, the m. *serratus ventralis* (2.93 N compared with 1.95 N in *T. europaea* and 4.29 N compared with 2.11 N in *T. aquitania*).

In general, we can notice that fossorial adaptations in moles tend towards a reduction of mobility at joints to the benefit of stability. Indeed, as the forces applying on the forelimb while digging are great it is necessary to prevent dislocation, above all in the shoulder joint due to the abduction of the humerus that generates the greatest part of the lateral-thrust power stroke force. Lin et al. (2019) also noticed that the expanded humeral trochlea and the enlarged humeral epicondyles prevent elbow joint dislocation during digging. These authors argue that the elbow must principally resist flexion during the digging strokes, which is consistent with our findings that elbow flexors represent approximately half of the estimated force produced by the elbow extensors.

As noticed previously, antagonist muscle groups can display huge differences in muscle characteristics, as for the elbow flexors/extensors. This is especially true for the humeral abductors and adductors, as the adductors represent only 1/10th of the MM and 1/4th of force-producing capacity of the abductors according to our results. Rose et al. (2013) find this difference surprising and indicated that the anterior superficial and deep muscle compartments of the m. *pectoralis major*, corresponding to what we call the m. *pectoantebrachialis*, might participate to humeral adduction rather than abduction, as already hypothesised by Reed (1951) and Yalden (1966). The m. *pectoantebrachialis* is a rather small muscle (weighting around 0.145 g and producing a force estimated between 3.1 and 3.6 N on average, Table S2) in comparison with all the other humeral abductors. Therefore, even with this muscle assigned to the humeral adductors, a gap between the two antagonist muscle groups remains both in terms of mass and estimated isometric force. The humeral abductor mass ranges from 59.3% to 56.3% of the total forelimb weight, while the humeral adductors mass ranges from 6% to approximately 9% in both species, still representing only 1/6th of the humeral abductors mass with the m. *pectoantebrachialis* included. The estimated isometric force-producing capacity decreases from 44 to 40 N in the humeral abductors and increases from 10.5 to 14.1 N in the humeral abductors of *T. europaea*. It decreases from 47 to 44 N in *T. aquitania*'s humeral abductors and increases from 9.5 to 12.9 N in the humeral adductors. Thus, the humeral adductor force-producing capacity still represents only 1/3th of the force-producing capacity of the humeral abductors.

The more massive and stronger functional groups correspond globally to those that participate in resisting the soil reaction forces during digging: the scapular adductors maintain the scapula towards the body midline, the humeral abductors generate the greatest part of the power stroke force, and the elbow extensors extend the elbow, and thus, the forearm, while resisting flexion induced by the soil. Therefore, we hypothesise that soil reaction forces require a greater force than that needed to bring the forelimb back to the body during the recovery stroke. This would explain the greater force-producing capacity of these muscle groups. Rose et al. (2013) and Lin et al. (2019) identified a particularly important role of the humeral abductors, the elbow extensors but also of the carpal flexors in the application of the forelimb high lateral out-force during digging for *S. aquaticus*. As said previously, we found carpal and digital extensors to be more massive and stronger than carpal and digital flexors for *T. europaea* and *T. aquitania*, making it particularly interesting to investigate variations in movements and locomotor performance during digging between these species.

4.4 | Inter and intraspecific variability in the two *Talpa* species

Despite general description of forelimb anatomy provided previously, and the great level of morphological convergence in *Talpa* species, anatomical dissections and the quantification of muscle features allowed us to highlight both an inter and intraspecific variability in muscle PCSA, and thus in muscle force-producing capacity. The existence of an inter- and intraspecific variability in *Talpa* species was previously shown using 3D geometric morphometric methods for two forelimb bones, the humerus and the ulna (Costes et al., 2023) and for the semicircular canals (Melekian et al., 2025). These two studies focused on the three sister species *T. europaea*, *T. aquitania*, and *T. occidentalis* and both found intraspecific variability in *T. aquitania* across sampling sites. No intraspecific variability was found in *T. europaea* for the forelimb bones and the inner ear. In the present study, sampling size did not allow us to test for an intraspecific variability in muscle architecture in *T. europaea*. However, we found that *T. aquitania* specimens were separated according to sampling sites along the first axis of the PCA (Figure 10), representing the greatest part of PCSA variation. Moreover, intraspecific variation in *T. aquitania* was found along the second axis of ulna and semicircular canal PCA representing a significant part of the variation for both these structures. Curiously, according to our results, the two most important muscle groups providing lateral out-force during the power stroke (i.e., the humeral abductors and elbow extensors), were not important contributors to explain the variations in the PCSA dataset. Conversely, shoulder extensors, scapular adductors,

elbow flexors, and carpal/digital flexors PCSA mainly structured variations at the interspecific level, while shoulder flexors, scapular protractors, as well as carpal/digital extensors mainly structured variations at the intraspecific level.

Lin et al. (2019), while comparing digging movement of *S. aquaticus* in compact and loose substrates, found stereotyped patterns of digging movements at the shoulder joint (involving movement of scapula and humerus), whereas there were substantial differences at the elbow (especially during late stage of forelimb retraction) and carpal joints. We can hypothesise that fully fossorial moles generate high force during digging always in the same way, this force generation relying principally on the action of the humeral abductors and, to a lesser extent, on the extension of the forearm performed by the elbow extensors. This might, thus, explain the weaker level of variation between the species and among the populations for these two muscle groups. Nonetheless, when we focused on these two muscle groups and on the humeral adductors, we found inter and intraspecific variation for the humeral adductors and the elbow extensors, and only intraspecific variation for the humeral abductors.

Focusing on the relationship between muscle group PCSA and the shape of the ulna and humerus, we were able to show that shoulder extensors, carpal/digital extensors and carpal/digital flexors PCSA were highly integrated with humerus shape and that elbow extensors PCSA were highly integrated with the ulna. Very few muscle functional groups showed significant covariation with bone shape, even though the r_{PLS} was rather high for each PLS. This is somewhat surprising for the humeral abductors and adductors that all insert on the humerus.

However, while investigating PCSA variation, we found, as expected, m. *teres major* PCSA to be higher in the *T. aquitania* population of Aveyron, following the *teres tubercle* shape variation (on the humerus) described by Costes et al. (2023). The m. *subscapularis* PCSA vector, although small and thus only weakly explaining variation on the second PCA axis (Figure 11), also shows higher values in *T. aquitania* specimens from Aveyron in accordance with humerus shape variation. Considering the humeral abductor PCSA, despite our results for the m. *teres major* and m. *subscapularis* at the intraspecific level, we found no interspecific variation, whereas interspecific shape variation of the humerus on insertion sites of these muscles was highlighted by Costes et al. (2023). We also did not find the mm. *pectorales*, that we divided in four muscles in our study, to have higher PCSA values in *T. europaea* as expected following description of humerus shape. Except for the intraspecific variation, our results are consistent with the non-significance of the PLS between the humerus shape and the PCSA of these muscles.

More surprisingly, we found the humeral adductors, and especially the m. *spinodeltoideus* PCSA being higher in *T. europaea*, consistent with the deltoid process of the humerus previously described as being larger in this species. Moreover, the two muscles assigned to the shoulder extensors, the m. *cleidodeltoideus* and the m. *acromiodeltoideus*, are also humeral adductors. This is all the more surprising as shoulder extensors' covariation with the humerus was significant but not the covariation with the humeral adductors. Therefore, we can suppose that our small sample size might have had an impact on the significance of the tests. Despite our small sample size, we found significant covariations between the shoulder extensor PCSA and the humerus shape and between the elbow extensors and the ulna, that both showed an inter and intraspecific structure on the first axis of the PLS. Bone shape variation along this axis of the two PLS graphs follows shape variations described by Costes et al. (2023) for each species and population.

Both shape variation and areas on the humerus that covary with the shoulder extensor PCSA involved a deltoid fossa that is more bulging in *T. aquitania* and deeper in *T. europaea* specimens. As PCSA values are greater in *T. europaea* specimens, we can suppose that a deeper deltoid fossa creates a greater space to insert these stronger muscles. For the elbow extensors, Costes et al. (2023) described a larger insertion site for the m. *triceps brachii* in *T. aquitania* and in *T. aquitania* specimens from Gironde. However, our anatomical dissections allowed us to identify insertion sites more precisely for each head of the triceps that we individualised. Therefore, we found the m. *triceps brachii caput laterale* PCSA to be higher in *T. europaea*, consistent with its insertion site on the humerus which was already described as larger by these authors. Here, we also showed that the medial side of the olecranon, where the muscle inserts on the ulna, is larger in *T. europaea*, both considering shape variation in Costes et al. (2023) and areas that covary with muscle PCSA (Figure 13). The m. *triceps brachii longum* and m. *triceps brachii mediale* PCSA are higher in *T. aquitania* and in Aveyron (and not Gironde) specimens at the intraspecific level, which is also consistent with the shape variation and covariation of the lateral side of the olecranon, being larger in this species and population. Covariation between the humerus shape and carpal/digital extensors only showed an inter and intraspecific structure on the second axis of the PLS and the covariation between the humerus shape and carpal/digital flexors showed no structure in either species or population. Therefore, another factor than « species » might explain part of these covariations.

Nonetheless, inter and intraspecific variation of the shoulder extensors, the elbow extensors, the carpal/digital extensors and their insertion sites on bones is mostly observed along the same axis of covariation, meaning that similar patterns drive macro- and microevolutionary patterns in these two *Talpa* species. In addition to bone shape variation and covariation patterns being nearly the same, our results confirm that bone shape is directly influenced by muscle volume and force (Brassard et al., 2020; Cornette et al., 2015). Interestingly, we generally found larger insertion sites correlated to higher PCSA values, thus to estimated muscle force. Variations in both forelimb anatomy and inner ear morphology suggest inter and intraspecific variations in locomotor performance in the two species. Indeed, semicircular canals play a crucial role in balance, while forelimb muscles provide motion and force during locomotion. Given the results of Lin et al. (2019) demonstrating that substrate compactness can impact movements during digging in fossorial moles, studying soil characteristics and their relationship to digging movements and performance might provide some explanation on the existence of these different morphological groups. Considering the intraspecific

variations, the phylogenetic analysis of Nicolas et al. (2017) of the Cytochrome b gene also highlighted genetic differences and revealed the presence of four sublineages within *T. aquitania*. As the two sublineages corresponding respectively to Gironde population and Aveyron population have an estimated divergence time of 0.349 ± 0.050 My, Melekian et al. (2025) argue that the genetic structuring can be explained by history of populations with allopatric differentiation occurring in multiple refugia during the Pleistocene. Consequently, the observed differences in bone and muscle anatomy may not be adaptive.

5 | CONCLUSION

In the present study, based on the anatomical dissections, we provided a redescription of 39 muscles inserting on all the forelimb bones, including the forearm, of *T. europaea* and *T. aquitania*. This work allowed us to provide a description of *T. aquitania* musculature, for which no data were available yet and that we did not find qualitatively different from that of *T. europaea*. As previous work already existed on *T. europaea*, we redescribed the species musculature in accordance with this literature and updated the nomenclature used for the muscles. Quantitative analyses performed on features of 36 of these muscles involved in forelimb motion highlighted inter and intraspecific (in *T. aquitania*) variations in muscle force-producing capacity. This is consistent with our expectations based on previous study of the inner ear and forelimb bones morphology, which already highlighted this variability in the two species. A functional explanation can be considered, as different constraints imposed by the different properties of their environments (soil compactness, plasticity, composition…) could have impacted forelimb morphology and locomotor mechanisms. Nevertheless, the subtle genetic divergences previously observed can be linked to these two mole species' evolutionary history, related to climatic oscillations creating multiple refugia during the Pleistocene, and could also explain the inter and intraspecific variations we observed. In this context, it would be interesting to further analyse soil properties in which each species, and each population of *T. aquitania*, move. A study investigating the kinematics of movement and locomotor performances during digging could also provide some highlights to better understand the specificity of their fossorial adaptations. Such a study could also provide some explanations for the differences we found between our work on the two *Talpa* species and previous works studying *S. aquaticus* musculature, which is another example of a fully fossorial mole.

AUTHOR CONTRIBUTIONS

E.K. and R.C. conceived and designed the study and performed the statistical analyses and interpretation of data. E.K. carried out the acquisition of data and drafted the manuscript. A. H. and C. H. contributed to collecting data and to interpretation of data. A. D. contributed to collecting data and segmented the 3D bones mesh used for the figures. V.N, M. P., and D. C. contributed to conception and design of the study. All authors revised and approved the manuscript.

ACKNOWLEDGMENTS

The authors would like to thank the Museum National d'Histoire Naturelle (MNHN) for access to the collection, with a special thanks to Lucile Armand. We are also grateful to recent field collectors who deposited their specimens in the collection of the Museum National d'Histoire Naturelle: Quentin Martinez, Yves Cambournac, Jean-Luc Laclamette, François Burgot, Bernard Métivier, and Jean-Pierre Hugot.

CONFLICT OF INTEREST STATEMENT

The authors declare no conflict of interest.

DATA AVAILABILITY STATEMENT

The data that support the findings of this study are available from the corresponding author upon reasonable request.

ORCID

Estelle Klein https://orcid.org/0009-0002-7404-7859
Anthony Herrel https://orcid.org/0000-0003-0991-4434

REFERENCES

Abe, H. (2001) Soil hardness, a factor affecting the range expansion of *Mogera wogura* in Japan. *Mammal Study*, 26, 45–52.

Adams, D.C., Collyer, M.L., Kaliontzopoulou, A. & Baken, E.K. (2021) "Geomorph: Software for geometric morphometric analyses. R package version 4.0.". .

Baylac, M. & Frieß, M. (2005) Fourier descriptors, Procrustes superimposition, and data dimensionality: an example of cranial shape analysis in modern human populations. In: *Modern morphometrics in physical anthropology*. Boston, MA: Springer, pp. 145–165.

Biewener, A. & Patek, S. (2018) *Animal locomotion*. Oxford, UK: Oxford University Press.

Böhmer, C., Theil, J.-C., Fabre, A.-C. & Herrel, A. (2021) *Atlas of terrestrial mammal limbs*, 1st edition. Boca Raton, FL: CRC Press.

Brassard, C., Merlin, M., Monchâtre-Leroy, E., Guintard, C., Barrat, J., Callou, C. et al. (2020) How does masticatory muscle architecture covary with mandibular shape in domestic dogs? *Evolutionary Biology*, 47(2), 133–151.

Campbell, B. (1939) The shoulder anatomy of the moles. A study in phylogeny and adaptations. *American Journal of Anatomy*, 64, 1–39.

Castiella, M.J., Laville, E., Renous, S. & Gasc, J.P. (1992) Caractéristiques Morphologiques Du Membre Antérieur de La Taupe Commune, *Talpa europaea* (Mammalia, Talpidae). *Mammalia*, 56(2), 265–286.

Cornette, R., Tresset, A. & Herrel, A. (2015) The shrew tamed by Wolff's law: do functional constraints shape the skull through muscle and bone covariation? *Journal of Morphology*, 276, 301–309.

Costes, P., Klein, E., Delapré, A., Houssin, C., Nicolas, V. & Cornette, R. (2023) Comparative morpho-functional analysis of the humerus and ulna in three Western European moles species of the genus *Talpa*, including the newly described *T. aquitania*. *Journal of Anatomy*, 00, 1–20.

Currey, J.D. (2002) *Bones: structure and mechanics*. Princeton, NJ, USA: Princeton University Press.

Currey, J.D. (2003) The many adaptations of bone. *Journal of Biomechanics*, 36, 1487–1495.

Edwards, L.F. (1937) Morphology of the forelimb of the mole (Scalopus aquaticus, L.) in relation to its fossorial habits. *Ohio Journal of Science*, 37, 20–24.
Fabre, A.C., Cornette, R., Goswami, A. & Peigné, S. (2015) Do constraints associated with the locomotor habitat drive the evolution of forelimb shape? A case study in musteloid carnivorans. *Journal of Anatomy*, 226(6), 596–610.
Freeman, R.A. (1886) Anatomy of the shoulder and upper arm of the mole (Talpa europaea). *Journal of Anatomy and Physiology*, 20(Pt 2), 200–201.
Gambaryan, P.P., Gasc, J.P. & Renous, S. (2002) Cinefluorographical study of the burrowing movements in the common mole, *Talpa europaea* (Lipotyphla, Talpidae). *Russian Journal of Theriology*, 1, 91–109.
Hartstone-Rose, A., Perry, J.M. & Morrow, C.J. (2012) Bite force estimation and the fiber architecture of felid masticatory muscles. *The Anatomical Record*, 295(8), 1336–1351.
Hugot, J.P., Gu, S.H., Feliu, C., Ventur, J., Ribas, A., Dormion, J. et al. (2014) Genetic diversity of *Talpa europaea* and Nova hanta virus (NVAV) in France. *Bulletin de L'academie Veterinaire de France*, 167(3), 4210–4267.
Hutchison, J.H. (1968) Fossil Talpidae (Insectivora, Mammalia) from the later tertiary of Oregon. *Bulletin of the Museum of Natural History, University of Oregon*, 11, 11.
Jullien, R. (1967) Musculature du Membre Antérieur chez les Principaux Types d'Insectivores. *Mémoires du Muséum National d'Histoire Naturelle*, 48, 1–68.
Klingenberg, C.P. (2016) Size, shape, and form: concepts of allometry in geometric morphometrics. *Development Genes and Evolution*, 226(3), 113–137.
Leonard, K.C., Worden, N., Boettcher, M.L., Dickinson, E. & Hartstone-Rose, A. (2022) Effects of freezing and short-term fixation on muscle mass, volume, and density. *The Anatomical Record*, 305(1), 199–208.
Lin, Y.F., Konow, N. & Dumont, E.R. (2019) How moles destroy your lawn: the forelimb kinematics of eastern moles in loose and compact substrates. *Journal of Experimental Biology*, 222(4), jeb182436.
Loeb, G.E. & Gans, C. (1986) *Electromyography for experimentalists*. Chicago, IL: The University of Chicago Press, p. 373.
Marchetti, L., MacDougall, M.J., Buchwitz, M., Canoville, A., Herde, M., Kammerer, C.F. et al. (2024) Origin and early evolution of vertebrate burrowing behaviour. *Earth-Science Reviews*, 250, 104702.
Martin, M.L., Travouillon, K.J., Fleming, P.A. & Warburton, N.M. (2020) Review of the methods used for calculating physiological cross-sectional area (PCSA) for ecological questions. *Journal of Morphology*, 281(7), 778–789.
Medler, S. (2002) Comparative trends in shortening velocity and force production in skeletal muscles. *American Journal of Physiology-Regulatory, Integrative and Comparative Physiology*, 283(2), R368–R378.
Melekian, A., Tarquini, S.D., Nicolas, V., Poulet-Crovisier, N. & Ladevèze, S. (2025) Morphometric study of the bony labyrinth of the inner ear in the European moles *Talpa europaea*, *Talpa occidentalis*, and *Talpa aquitania*. *Journal of Anatomy*, 00, 1–11.
Mendez, J. & Keys, A. (1960) Density and composition of mammalian muscle. *Metabolism*, 9, 184–188.
Murdoch, D. & Adler, D. (2021) "Rgl: 3D visualisation using OpenGL. R package version 0.108.3.". https://CRAN.R-project.org/package=rgl
Nevo, E. (1979) Adaptive convergence and divergence of subterranean mammals. *Annual Review of Ecology and Systematics*, 10, 269–308.
Nicolas, V., Hugot, J.P. & Cornette, R. (2021) New data on the distribution of the two mole species *Talpa aquitania* Nicolas, Martínez-Vargas & Hugot, 2017 and *T. Europaea Linnaeus*, 1758 in France based on museum and newly collected specimens. *Zoosystema*, 43(24), 585–617.
Nicolas, V., Martinez-Vargas, J. & Hugot, J.P. (2017) Molecular data and ecological niche modelling reveal the evolutionary history of the common and iberian moles (Talpidae) in Europe. *Zoologica Scripta*, 46, 12–26.
Polly, P.D. & Hall, B.K. (2007) Limbs in mammalian evolution. In: *Fins into Limbs: Evolution, Development, and Transformation*. Chicago, IL: University of Chicago Press, pp. 245–268.
R Core Team. (2024) "R: a language and environment for statistical computing. Vienna, Austria: R Foundation for Statistical Computing.". https://www.R-project.org/
Reed, C.A. (1951) Locomotion and appendicular anatomy in three soricoid insectivores. *American Midland Naturalist*, 45, 513–671.
Rohlf, F.J., Loy, A. & Corti, M. (1996) Morphometric analysis of old world Talpidae (Mammalia, Insectivora) using partial-warp scores. *Systematic Biology*, 45, 344–362.
Rose, J.A., Sandefur, M., Huskey, S., Demler, J.L. & Butcher, M.T. (2013) Muscle architecture and out-force potential of the thoracic limb in the eastern mole (*Scalopus aquaticus*). *Journal of Morphology*, 274(11), 1277–1287.
Rothier, P.S., Fabre, A.C., Clavel, J., Benson, R.B. & Herrel, A. (2023) Mammalian forelimb evolution is driven by uneven proximal-to-distal morphological diversity. *eLife*, 12, e81492.
Schlager, S., Zheng, G., Li, S. & Szekely, G. (2017) Morpho and Rvcg-shape analysis in R. In: *Statistical Shape and Deformation Analysis*. London: Academic Press, pp. 217–256.
Sharir, A., Stern, T., Rot, C., Shahar, R. & Zelzer, E. (2011) Muscle force regulates bone shaping for optimal load-bearing capacity during embryogenesis. *Development*, 138, 3247–3259.
Taverne, M., Fabre, A.C., Herbin, M., Herrel, A., Peigné, S., Lacroux, C. et al. (2018) Convergence in the functional properties of forelimb muscles in carnivorans: adaptations to an arboreal lifestyle? *Biological Journal of the Linnean Society*, 125(2), 250–263.
Whidden, H.P. (2000) Comparative myology of moles and the phylogeny of the Talpidae (Mammalia, Lipotyphla). *American Museum Novitates*, 3294, 1–53.
Wilson, D.E. & Mittermeier, R.A. (2018) "Handbook of the mammals of the world: vol. 8: insectivores, sloths and colugos.".
Woledge, R.C., Curtin, N.A. & Homsher, E. (1985) Energetic aspects of muscle contraction. *Monographs of the Physiological Society*, 41, 1–357.
Wolff, J. (1892) *Das Gesetz der Transformation der Knochen*. Berlin: August Hirschwald Verlag.
Yalden, D.W. (1966) The anatomy of mole locomotion. *Journal of Zoology*, 149(1), 55–64.

SUPPORTING INFORMATION

Additional supporting information can be found online in the Supporting Information section at the end of this article.

How to cite this article: Klein, E., Herrel, A., Houssin, C., Delapre, A., Nicolas, V., Chablat, D. et al. (2026) Musculoskeletal variation in the forelimb of two highly specialised diggers (genus *Talpa*). *Journal of Anatomy*, 00, 1–23. Available from: https://doi.org/10.1111/joa.70201